Terrace formation linked~~coupled~~ to outburst floods at the Diexi palaeo-landslide dam, upper Minjiang River, eastern Tibetan Plateau

Jingjuan Li[1], John D. Jansen[2], Xuanmei Fan[1], Zhiyong Ding[1], Shugang ~~Kang[2]~~Kang[3], Marco Lovati[1]

[1] State Key Laboratory of Geohazard Prevention and Geoenvironment Protection, Chengdu University of Technology, Chengdu 610059, China
[2] GFÚ Institute of Geophysics, Czech Academy of Sciences, Prague, Czechia
~~2~~ [3] State Key Laboratory of Loess and Quaternary Geology, Institute of Earth Environment, Chinese Academy of Sciences, Xi~~'~~'an 710061, China

Correspondence to: Xuanmei Fan (fxm_cdut@qq.com)

Abstract

River terraces are frequently investigated with the aim of extracting information regarding tectonic or climate forcing on the evolution of landscapes~~Tectonic uplift and climate changes are the two critical factors that control the evolution of river landscapes and the formation of terraces~~. Terraces formed following the b-lockage of valleys by large-scale landsliding ~~has~~have received limited attention despite the high likelihood of their prevalence in landslide-dominated mountain belts. H~~owever, the effect of river blockage events on terrace formation along valley areas remains poorly understood. In this paper~~ere, we investigate~~d~~ the geomorphology, sedimentology, and chronology of ~~the~~ two outstanding sets of terraces upstream of the giant, river-blocking Diexi palaeo-landslide on the upper Minjiang River, eastern Tibetan Plateau. The first set occurs at Tuanjie village and has seven levels (T1-T7); the second set, at ~~terraces at the Tuanjie village (seven staircases) and at the~~ Taiping village, has three levels (T1-T3) ~~(three staircases) in the Diexi area. These represent two typical fluvial terraces in the upper Minjiang River in the eastern Tibetan Plateau~~. All the terraces display a consistent sedimentary sequence comprising lacustrine muds topped by fluvial gravels sometimes capped by ~~a~~ loess and~~-rich~~ a palaeosol. Based on ~~These terraces are composed, from bottom to top, of lacustrine deposits, gravels, loess, and paleosol.~~ f~~F~~ield ~~investigation~~examination, lithofacies analysis, ~~Digital Elevation Model (DEM)~~elevation data, ~~lithofacies,~~ and ~~dating results~~chron~~ol~~o~~gical~~metric data (optically stimulated luminescence and radiocarbon dating), we ~~confirm that terraces~~correlate T1, T2 and ~~to~~ T3 at Taiping ~~in Taiping correspond to~~with ~~terraces~~ T5, T6 and ~~to~~ T7 ~~in~~ at Tuanjie. Our ~~findings~~ analysis suggests two damming and four three outburst events events have occurred in the areaat the Diexi palaeo-landslide since the Late Pleistoceneover the past 35,000 years. A giant The palaeo-landslide (>300 m high)dam blocked the river before 32 35 ka, followed by the first outburst flood at ~ 27 ka; the river was blocked . Then, the palaeo-dam blocked the river again between 27 to 17 ka, and suffered followed by a second dam-breaking eventoutburst at ~17 ka; and a third outburst . The third and fourth progressive collapse events, respectively, occurred at ~10 12 ka was followed by gradual fluvial incision of the palaeo-dam crest to its current level and ~9 ka. –We attribute the terraces at Diexi to the recurrent blockage and outburst events, which reflect the shifting sediment transport capacity and incision at the palaeo-dam crest. Here, climatic fluctuations play a minor role in terrace formation, and tectonism plays no role at all.Our analysis, combined with the tectonic uplift rate, river incision rate, and high-resolution climate data, indicates that the blockage and collapse of the palaeo-dam have been a significant factor in the formation of the river terraces in the tectonically active mountainous region. Tectonic movement and climatic fluctuations, on the other end, play a minor role.

1 Introduction

TerracesRiver terraces are temporary sediment storages along valleys that provide a , as a natural archive of information on –the process of sediment transport and deposition through timevalley evolution, are used to explore the controlling mechanisms of river landscapes (Chen et al., 2020; Liu et al., 2021), processes that are typically . This landform is sensitive to the impacts of tectonics tectonism and climate (Pan et al., 2003; Singh et al., 2017; Avsin et al., 2019; Gao et al., 2020; Do Prado et al., 2022). It Terraces can have been shown to reflect a wide range of geomorphic controls, such as reflect the dynamics of the fluvial system (Schumm and Parker, 1973), rock uplift rate (Jansen et al., 2013; Pan et al., 2013; Giano and Giannandrea, 2014; Malatesta et al., 2021), fault activity (Caputo et al., 2008), crustal movement flexure (Yoshikawa et al., 1964; Westaway and Bridgland, 2007; Okuno et al., 2014), glacier melting (Bell, 2008; Oh et al., 2019; Vásquez et al., 2022), changes in sediment supply (Jansen et al., 2011), sea level (Yoshikawa et al., 1964; Malatesta et al., 2021), and– even the internal dynamics of the fluvial system (Schumm and Parker, 1973)lake level changes (Wang et al., 2021b). In tectonically-active mountainouss regions, , some extreme events like large-scale landslides, debris flows, and rockfalls ~~also change fluvial dynamics and landscapes~~ (Molnar et al., 1993; Molnar and Houseman, 2013; Srivastava et al., 2017) can cause ~~. Among these events,~~ river blockages and associated sudden outburst floods~~s~~ ~~can strongly affect the~~that have a major impact on the sedimentary processes ~~evolutionary and geomorphology~~ of the upstream and downstream ~~sections~~ reaches, including terrace formation (Korup et al., 2007; Hewitt et al., 2008; Korup et al., 2010; Hewitt et al., 2011). And yet, ~~Currently, there are~~ few studies have explored ~~on~~ the influence of ~~disaster~~ extreme events on the formation and evolution of terraces (Montgomery et al., 2004; Yuan and Zeng, 2012; Zhu et al., 2013; Chen et al., 2016; Arzhannikov et al., 2018; Hu et al., 2018; Arzhannikov et al., 2020; Xu et al., 2020). We attempt to address that knowledge gap here.~~, and further exploration is advisable.~~

~~The r~~Rapid uplift and climate change ~~of the Tibet~~during~~an Plateau in~~ the ~~late~~ Quaternary have led to frequent extreme geomorphic ~~extremedisaster~~ events ~~in its~~in the area drained by the Minjiang River at the eastern margin of the Tibetan Plateau ~~,~~(Gorum et al., 2011; Fan et al., 2017; 2018; Wu et al., 2019; Dai et al., 2021; Yang et al., 2021). The upper Minjiang, for instance, displays many terrace sequences ~~As a result, the formation factors of river terraces in this region have been controversial,~~ with origins that remain debated ~~and the causes of the periodicity of the orbital scale (100 ka, 40 ka, 20 ka) and centennial-scale (0.1 ka) are also unclear.~~

~~The upper Minjiang River is located in the eastern Tibetan Plateau, and a wide distribution of three-tiered terraces characteriz~~s~~es characterises it~~ (Yang, 2005). But ~~The development of palaeo-landslides, climate variations, and the movement and evolution of regional tectonic uplift have been studied through these terraces.~~ d~~D~~ue to the lack of detailed sedimentological, chronological and geomorphological information ~~along the upper Minjiang River,~~ the role of extreme geomorphic events, ~~the studies on the development of~~ such as landslides and outburst floods, ~~palaeo-landslide, climate variations and regional tectonic uplift~~ are still being explored ~~, incompleteness of relevant data, these studies are still exploratory~~ (Yang et al., 2003; Yang, 2005; Gao and Li, 2006; Zhu, 2014; Luo et al., 2019).

~~The~~ A set of outstanding terraces occur just upstream of~~terraces in the Diexi area are typical fluvial terraces in the upper Minjiang River, and they are located in~~ the ~~famous~~ 300 m-high Diexi palaeo-landslide ~~palaeo-~~dam~~med lake~~, ~~which is~~ one of the largest, best-preserved, and longest-duration landslide-dammed lakes in a tectonically-~~-~~active ~~mountainous region~~setting (Fan et al., 2019). ~~Previous studies found two terraces developed in Tuanjie and Taiping villages (Fig. 1)~~ (!!! INVALID CITATION !!! (Wang et al., 2005b; Yang et al., 2008; Fan et al., 2019))~~. The analysis of lithofacies and sedimentary~~

systems determined that the Diexi area is mainly composed of fluvial, lacustrine, alluvial fan and eolian sedimentary systems (Yang, 2005; Yang et al., 2008).The Diexi terraces (Fig. 1) have been examined by previous workers –Previous studies foundThere are two terraces developed inat Tuanjie and Taiping villages in the Diexi area (Fig. 1) (Wang et al., 2005a; Yang et al., 2008; Fan et al., 2019)., Unfortunately,but the a systematic sedimentological study of the Tuanjie and Taiping Terraces' terracessedimentary facies is incompletestill unclearanalysis has yet to be conducted. A set of terraces at the village of Tuanjie Currently,is –Tuanjie Terraces are thought to have resulted from via the repeated outburst floods of from the a Diexi palaeo-dammed lake –between 30 and 15 ka000 years ago , and each terrace corresponds corresponding to a different stages of outburst (Duan et al., 2002; Wang et al., 2005b; Wang, 2009; Zhu, 2014; Ma et al., 2018). This indicates that the Diexi palaeo-dammed lake has experienced more than one outburst flood event (Wang et al., 2005b; 2012; Ma et al., 2018). At least two blockage events have also been suggested Moreover, the sedimentological analysis also suggests that the Diexi palaeo-dammed lake experienced at least two periods of blocking and outburst events (Yang, 2005; Yang et al., 2008) together with, and four periods of fluvial progradation (Xu et al., 2020). However, mechanistic details of the terrace formational processes based on the sedimentology and a comprehensive dating analysis are lacking. Here, we seek to address the unresolved questions of the origins of the Diexi terraces, including the following aimsDue to the lack of sedimentary sequence and chronological data, further study on the evolution of palaeo-dam and the causes of terrace formation is needed. The roles of tectonic activity, climate, river blockage and outburst events are crucial for discussing the formation of terrace staircases.

To explore the unsolved problems mentioned above, we investigated the geomorphological and sedimentological characteristics of the Tuanjie and Taiping Terraces using two independent dating methods, optically stimulated luminescence (OSL) and radiocarbon. The purposes of this paperour research are: (1) to complement theconduct a detailed analysis of terrace sedimentology; (2) to obtain absolute depositional ages of the terraces (at ical and chronological evidence of the Tuanjie and Taiping) terraces; and (23) to exploreunderstand the evolution ary process of the Diexi palaeo-dam since its formation at more than 35 ka (Wang etal., 2020). Our broader objective is to provide a better understanding terrace formation linkcoupled to extreme geomorphic events in mountain regions.These provide fundamental information for analysing the impact of tectonics, climate, and geological extreme events on the formation of terraces.(1) to clarify the deposition ages and sedimentary characteristics of

Taiping and Tuanjie terraces; (2) to reveal the blockage and outburst of the palaeo-dam; (3) to explore the influences of tectonics, climate, and geological disasters (blocking and damming) on the formation of terraces.

2 Study area

The The Diexi palaeo-landslide dam area is located on the eastern Tibetan Plateau in the upper reaches of the Minjiang River. The area exposes, which rocks belongs toof the northeast margin of the Tethys Himalayan domain and the Barkam formation zone, on the eastern margin part of the Bayan Har Block (Fig. 1a), . spanning the The area features visible strata from various periods: Devonian, Carboniferous, Permian, Triassic, and Quaternary periods (An et al., 2008; Zhang et al., 2011; Ma, 2017; Zhong, 2017). This region of the Tibetan Plateau has been affected by intense and frequent earthquakes (Yang et al., 1982; Chen and Lin, 1993; Li and Fang, 1998; Shi et al., 1999; Hou et al., 2001; Lu et al., 2004) linked to the ongoing collision of the Indian and Eurasian plates (Fig. 1b).

The Diexi study has an arid to semi-arid climate (Shi, 2020), with a strong effect of the prevailing winds. Cumulative evaporation averages 1000–1800 mm/y (Yang, 2005), and mean temperature and precipitation are 13.4℃ and 500–600 mm/y, respectively. Vegetation patterns show major elevational zonation and comprise mainly of mountain coniferous forests, alpine meadows, and low shrubs at the highest elevations.

TThe he Minjiang Valley valley is narrower at higher altitudes, and gradually widens downstream, overall, varying . The width of the valley bottom varies from 60 to 300 m wide at the valley floor (Yang, 2005; Jiang et al., 2016; Ma, 2017; Zhang, 2019), (Yang, 2005; Jiang et al., 2016; Ma, 2017; Zhang, 2019), and up to 3000 m deep flanked by steep hillslopes that are typically 30-35° and the steep slopes on both sides of the river valley have a gradient of 30-35° (Zhang et al., 2011; Guo, 2018), with a depth of 800 to 3000 m. The Many outburst sediments are deposited downstream of Diexi, such as in the Xiaoguanzi, Shuigouzi, and Manaoding villages (Fig. 1b).

Diexi palaeo-dammed lake (31º26′–′–33º16′ N; 102º59′–104º14′ E) is situated on the bend of the V-shaped Minjiang valley, which in turn lies in the well-known "‘north-south earthquake tectonic zone"’ (Tang et al., 1983; Huang et al., 2003; Yang, 2005; Deng et al., 2013).

TThehe Diexi palaeo-landslide that formed the Diexi palaeo-lake is located on the left bank of the

Minjiang River, from theat Jiaochang to the Diexi ancient townvillage (Fig. 1b). The palaeo-landslide .length and width are ~ 3500 m and 3000 m, respectively, and volume is ~ 1.4 to 2.0 km^3 (Zhong et al., 2021). The highest parts of the palaeo-landslide reach up to 3390 masl (metres above sea level), whereas the elevation of the dam crest is ~ 2500 masl (Dai et al., 2023).The highest elevation of the palaeo-landslide crown is 3390 m, and the main slide direction is SW18°. The length and width of the palaeo-landslide are about 3500 m and 3000 m, respectively, with a volume of the accumulation reaching 1.4 to 2.0×10^9 m^3 (Zhong et al., 2021). The elevation of the palaeo-landslide dam crest is 2500 m (Dai et al., 2023).

Diexi is located in the eastern Tibetan Plateau, and is being forged in the collision of the Indian and Eurasian plates (Fig. 1b). As the Tibetan Plateau and its surrounding areas have been affected by intense and frequent earthquakes during the late Quaternary (Yang et al., 1982; Chen and Lin, 1993; Li and Fang, 1998; Shi et al., 1999; Hou et al., 2001; Lu et al., 2004), Lake Diexi area is influenced by active and accelerated tectonic activity. The area features visible strata from various periods: Devonian, Carboniferous, Permian, Triassic, and Quaternary (An et al., 2008; Zhang et al., 2011; Ma, 2017; Zhong, 2017). The Songpinggou River flows eastward as a tributary of the Minjiang River and merges into the Minjiang River in Lake Diexi. It has a typical alpine erosion landform with an elevation of 1868-4800 m elevation. Large amounts of Quaternary lacustrine sediments are deposited along the Songpinggou river bedRiver.

At Taiping village (32º12′ N, 103º45′ E), three terraces occur near the mouth of Luobogou Gully (Fig. 1d) (Wang et al., 2005b; Fan et al., 2021), while a The climate of the entire region is monsoonal, being influenced by the Plateau Monsoon, the Westerlies, and the East Asian Monsoon. The Diexi Valleyarea, due to atmospheric circulation and the mountainous character, shows an arid and semi-arid climate (Shi, 2020). In the Diexi area, with the strong effect of the prevailing winds, the annual cumulative evaporation can reach 1000-1800 mm (Yang, 2005), and the average temperature and precipitation are 13.4℃ and 500-600 mm, respectively. Regarding ecological pattern, the vegetation shows a visible vertical zonation, composed mainly of mountain coniferous forests, alpine meadows, and low shrubs. The Songpinggou areas are scattered with forests of mountain pinus tabulaeformis, Sichuan-Yunnan alpine oak evergreen shrubs, and forests of deciduous species such as poplar and birch (Shi, 2020).

~~——The~~suite of seven terraces occurs 12 km downstream ~~staircases are located in~~ at Tuanjie village (32º2′ N, 103º40′ E) ~~are located in Tuanjie village~~ near ~~, on the right bank of the Minjiang River, at~~ the mouth of the Songpinggou tributary (Fig. 1c). Further downstream, high-energy gravel outburst deposits occur at scattered locations, including ~~The three terrace staircases are in Taiping village (32º12′13″ N, 103º45′53″ E), at the mouth of Luobogou Gully, which is 12 km upstream of the Tuanjie (Fig. 1d)~~ (Wang et al., 2005b; Fan et al., 2021)~~. –~~ near the villages of ~~From Taiping to Manaoding, the river has carved a deep canyon~~ ~~The course of the river from Taiping to Manaoding is a deep canyon (Duan, 2002), despite the Taiping and Tuanjie areas being have a broad valley landform.~~ ~~Many outburst sediments are deposited downstream of Diexi, such as in the~~ Xiaoguanzi, Shuigouzi, and Manaoding ~~villages~~ (Fig. 1b).

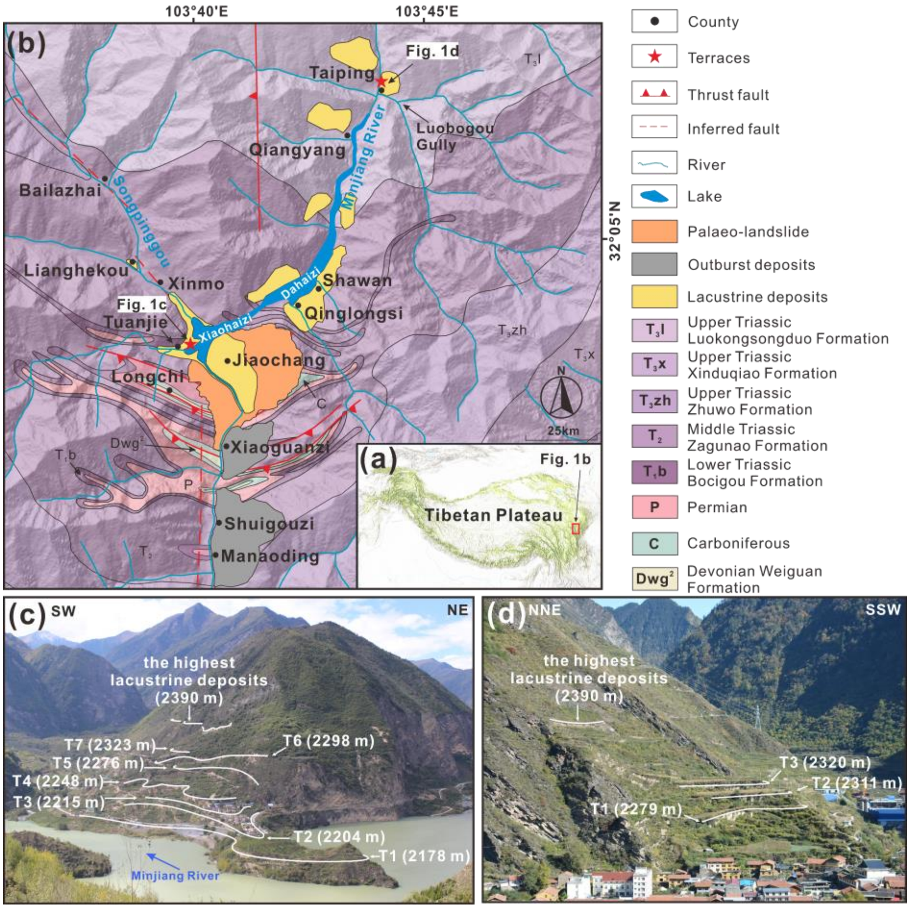

Figure 1. The Diexi study area. (a) Location of Diexi at the eastern margin of the Tibetan Plateau. (b) Geological setting (maps modified from Guo, 2018; Wang et al., 2020a; Zhong et al., 2021). (c) Oblique view of the seven Tuanjie terraces, including elevations (masl). (d) Oblique view of the three Taiping terraces including elevations (masl).

3 Materials and methods

3.1 Geomorphic and sedimentary description

F~~From October to November 2018, f~~ield surveys were carried out~~ in the Diexi area~~ from October to November 2018. ~~These terraces are named in order of Terrace 1 (T1) to Terrace 7 (T7) from bottom to top.~~ We described ~~The~~ sedimentary structure, geometric shape, sorting, roundness, and ~~the~~ palaeo-flow direction of the gravels by applying ~~-are described. The~~the lithofacies ~~of the Diexi palaeo-dammed lake were analyzsed analysed using the classification~~ approach primarily based on ~~method of sedimentary facies~~ Miall (2000), but also including~~ and~~ previous ~~research~~ work conducted by~~ in the Diexi area~~ Yang (2005) and Yang et al. (2008) (Table. 1). The terraces were numbered according to elevation from the lowermost terrace (T1) to higher terraces (Tn).

Terrace elevations were measured using Light Detection And Ranging (LiDAR) data with ~ 0.5 m vertical accuracy and the Advanced Spaceborne Thermal Emission and Reflection Radiometer Global Digital Elevation Model (ASTER GDEM) with ~ 30 m vertical accuracy (Fan et al., 2021).

~~These terraces are named in order of Terrace 1 (T1) to Terrace 7 (T7) from bottom to top.~~

Table. 1 Lithofacies of terrace sediments at Diexi. Adapted from Miall (2000), Yang (2005) and Yang et al. (2008).

Lithofacies code	Lithofacies	Sedimentary structures	Interpretation
Ps	Palaeosol	Pedogenic features, roots	Pedogenesis
Ls	Sandy loess	Massive texture	Eolian deposits
Gmm	Matrix-supported, massive gravel	Weak grading	Plastic debris flow (high-strength, viscous)
Gh	Clast-supported, crudely bedded gravel	Horizontal bedding, imbrication	Longitudinal bedforms, lag deposits, sieve deposits
Gci	Clast-supported gravel	Inverse grading	Clast-rich debris flow (high strength), or pseudoplastic debris flow (low strength)
Gcm	Clast-supported, massive gravel	-	Pseudoplastic debris flow (inertial bedload, turbulent flow)
Fm	Mud	snail shells	Overbank, abandoned channel, or drape deposits
Fl	silty clay	parallel bedding, wave bedding	Lacustrine deposits

3.2 Chronology

Two independent dating methods: ~~–~~optically stimulated luminescence (OSL) and radiocarbon dating, were employed to establish a reliable chronostratigraphic framework for the Tuanjie and Taiping terraces: OSL and radiocarbon. We collected samples from the top of the lacustrine and gravel units, and from the base of the loess and palaeosol units with the aim of To clarifying the timing of the damming and outburst processes of the palaeo-dam, and terrace the stabilityy:y time of terraces, we collected samples from the top of lacustrine and gravel units, and the bottom of loess and paleosol units. A total of twenty-two samples were obtained from the Tuanjie and Taiping terraces, including nineteen OSL samples samples and three radiocarbon samples in total . Of these, nineteen have been dedicated to OSL dating, while the other three have been allocated to radiocarbon dating (Figs. 2 and 3).

3.2.1 OSL dating

Nineteen OSL samples were collected from lacustrine deposits, gravel units, loess, and paleosol (Fig. 2 and 3). In At the Tuanjie Terraceterraces, twelve samples were collected taken from the lacustrine deposits (, excluding T6 and the highest lacustrine deposits); t. Two samples were collected from the gravel units of T2 and T5, and samples were taken from the paleosolpalaeosols samples were taken from theat T1 to T5 and T7 terraces (Figs. 2 and 3). In At the Taiping Terraceterraces, four samples were taken from the lacustrine deposits at the T1 to T3 terraces and the highest deposits, and another one was taken from the paleosolpalaeosol unit at the T3 terrace (Figs. 2 and 3). Samples were collected from freshly dug exposures, inserting To ensure that human activities and modern weathering did not disturb the samples, we scraped the surface sediments, and pushed the stainless steel tubes with a hammer to collect shielded depositsfollowed by careful sealing from light.. After the tubes were took out from the fresh sections, both ends of the tube were sealed with black opaque tape.

Samples were processed and measured at the Institute of Earth Environment, Chinese Academy of Sciences. The quartz grains were extracted following the standard laboratory pre-treatment procedures (Kang et al., 2013; 2020). The sediment at the tube-endss at the two ends of the tubes, , which may have been exposed to daylight during sampling, were removeddiscarded a. And, the unexposed samples were prepared for equivalent dose (D_e) and environment dose rate determination. Approximately 50 g samples were treated with 30% HCl and 30% H_2O_2 to remove carbonates and organic matter, respectively. Then, the samples were then washed with distilled water until the pH value of the solution reached 7. For samples IEE5542 and IEE5550, the coarse fractions (90-150 μm) were sieved out and etched with 40% HF for 45 mins, followed by washing using 10% HCl and distilled water. For the other 17 samples, the fine polymineral grains (4-11 μm) were separated according to the Stokes' law. These fine polymineral grains were immersed in 30% H_2SiF_6 for 3-5 days in an ultrasonic bath to extract quartz ~~.~~ Finally, the purified fine (coarse) quartz was deposited (mounted) on stainless steel discs with a diameter of 9.7 mm ~~for experimental use~~. The purity of quartz was verified by IRSL intensity and OSL IR depletion ratio (Figs. S1 and S2a; Duller, 2003).

All OSL measurements were performed on a Lesxyg Research measurement system, with blue light at (458 ± 10) nm, and infrared light at (850 ± 3) nm for stimulation and a $^{90}S/^{90}Y$ beta source (~0.05 Gy/s) for irradiation. Luminescence signals were detected by an ET 9235QB photomultiplier tube (PMT) through a combination of U340 and HC340/26 glass filters.

The single-aliquot regenerative-dose (SAR) protocol (Table. S1; Murray and Wintle, 2000; Wintle and Murray, 2006) was ~~utilizsed~~ utilised to determine the Equivalent Dose (D_e)~~,~~ ~~as used in~~following Kang et al. (2020). Quartz grains were preheated at 260°C for 10 s for natural and regenerative-dose, and a cut-heat at 220°C for 10 s was applied for the test dose. The quartz was stimulated for 60 s at 125°C with blue LEDs; t~~. T~~he OSL signal was calculated as the integrated value of the first 0.5 s of the decay curve minus the integrated value of the last 0.5 s as the background. For D_e determination, approximately 10 aliquots were measured for each sample. ~~And, t~~The mean D_e value of all aliquots was used as the final D_e value. Conventional tests in SAR protocol, including recuperation ratio, recycling ratio, quartz OSL brightness and fast-component dominated nature, growth curve shape, and D_e distribution (Figs. S2 and S3), indicated that the protocol ~~can be robustly used~~is adequate ~~to date~~for the samples in this study.

The environmental dose rate was estimated from the radioisotope concentrations (~~uranium~~U, ~~thorium~~Th, and ~~potassium~~K) and cosmic dose rates. U and Th concentrations were determined by inductively coupled plasma mass spectrometry ~~(ICP-MS)~~, while K concentration was measured by inductively coupled plasma optical emission spectrometry ~~(ICP-OES)~~. The cosmic dose rates were calculated using the equation proposed by Prescott and Hutton (1994). The α-value of fine-~~-~~grained (4-11 μm) ~~grained~~ quartz was assumed to be 0.04 ± 0.002 (Rees-Jones, 1995). Considering the sedimentary texture, and current and past climate conditions ~~, the sedimentary facies, and past climate changes~~ since ~~the sample~~ deposition, the water content of the gravel and ~~paleosol~~palaeosol was assumed to be 10 ± 5%, while the water content of lacustrine deposits was estimated to be 20 ± 5%. Dose rate was calculated using the Dose Rate and Age Calculator (DRAC) (Durcan et al., 2015). Finally, the quartz OSL ages were obtained by dividing the measured D_e (Gy) by the environmental dose rate (Gy/ka).

3.2.2 Radiocarbon dating

Three samples (all bulk sediment) were ~~obtained~~ collected for radiocarbon analysis: ~~, including~~ two ~~samples~~ from the highest lacustrine deposits in the Tuanjie and Taiping Terraces, and one ~~sample~~ from the ~~overlying~~ loess cap ~~of the~~at T4~~, terrace in~~ Tuanjie (Figs. 2 and 3). The ~~AMS~~radiocarbon ~~– ^{14}C~~ sample collected from the highest lacustrine deposits ~~of the~~at Taiping ~~village~~ was used ~~for~~ to compare~~ison~~ with the OSL sample (TP19-1) ~~, which was~~ taken from the same position. The ~~-~~radiocarbon samples ~~The AMS ^{14}C sample~~ collected from the highest lacustrine deposits ~~of the~~at Tuanjie ~~village~~ and the equivalent at Taiping ~~was~~ were compared~~. with the AMS ^{14}C dating of the highest lacustrine deposits of the Taiping village.~~ ~~Utiliz~~ s~~ing~~ Utilising the same dating method for age comparison enhances ~~credibility~~the robustness of our analysis. We sampled the ~~Field investigations showed that As the~~ loess unit ~~of the~~at Tuanjie T4, as it was the most complete and ~~easier~~ easiest to access.~~ collect, therefore, we collected the loess sample from the T4. The surface sediments were removed to avoid the influence of weathering.~~

All ~~the~~ samples were tested for ~~for the~~ organic matter, and ~~analyz~~s~~ed~~ analysed using the NEC accelerator mass spectrometer and ~~Thermo~~ thermo infra-red mass spectrometer at the Beta Analytic Radiocarbon Dating Laboratory~~. The samples were pre-treated following their protocols (REF)~~. All radiocarbon ages reported here are calibrated using ~~The ages were then converted into calendar years using the~~ IntCal 20 ~~calibration curve~~ (Reimer et al., 2020).

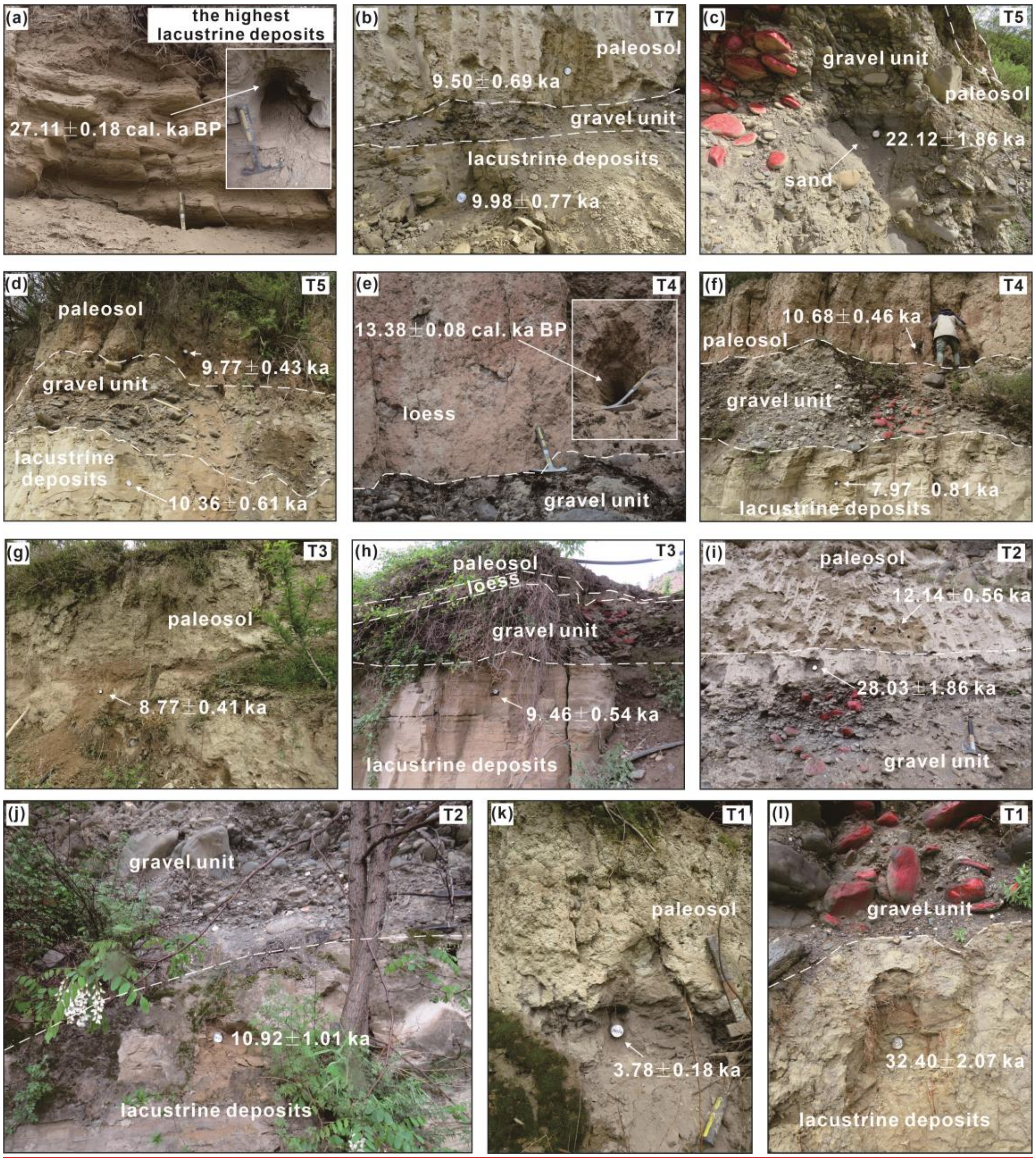

Figure 2. OSL and calibrated radiocarbon (denoted as cal. ka BP) dating results from Tuanjie. (a) The highest lacustrine deposits. (b) Lacustrine deposits and palaeosol at T7. (c) Gravel unit at T5. (d) Lacustrine deposits and palaeosol at T5. (e) Loess at T4. (f) Lacustrine deposits and palaeosol at T4. (g) Palaeosol at T3. (h) Lacustrine deposits at T3. (i) Gravel unit and palaeosol at T2. (j) Lacustrine deposits at T2. (k) Palaeosol at T1. (l) Lacustrine deposits at T1. White dashed lines mark unit boundaries.

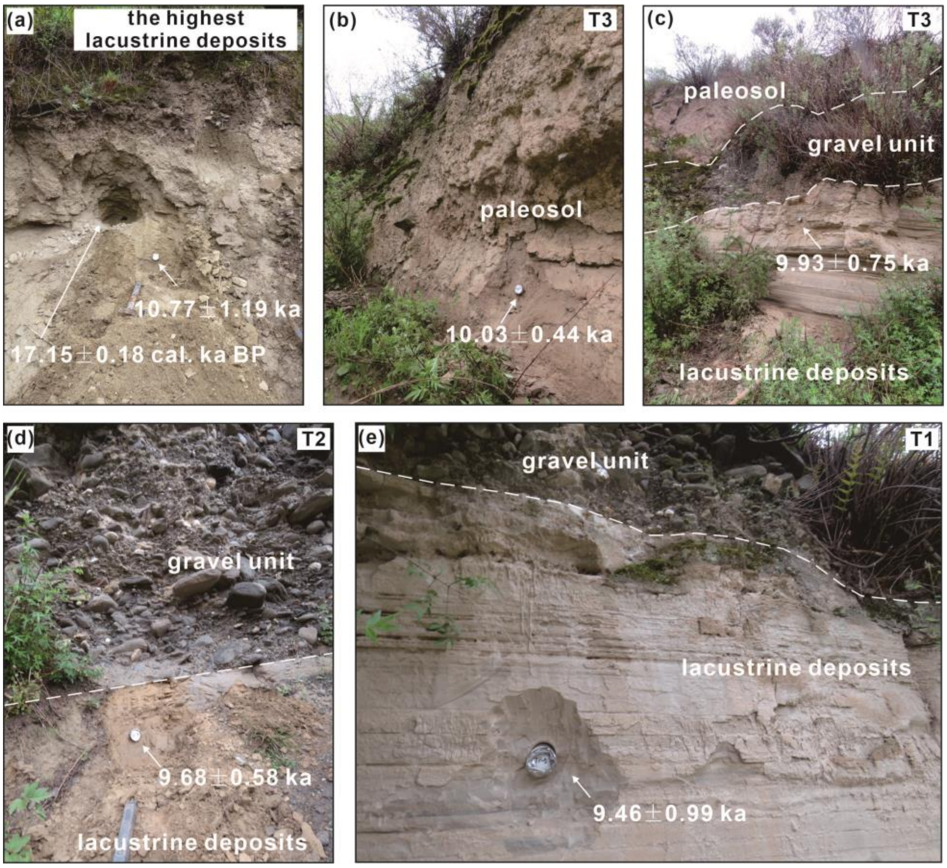

Figure 3. OSL and calibrated radiocarbon (denoted as cal. ka BP) dating results from Taiping. (a) Paired OSL and radiocarbon samples collected from the highest lacustrine deposits. (b) Palaeosol at T3. (c) Lacustrine deposits in T3. (d) Lacustrine deposits at T2; (e) Lacustrine deposits at T1. White dashed lines mark unit boundaries.

4 Results

4.1 Terrace~~s~~ geometry and distribution

The seven terraces at Tuan~~a~~jie ~~Terraces~~ and three terraces at~~have seven staircases,~~ Taiping Terraces ~~have three staircases, all of which they are~~are all developed on thick ~~–based on~~ lacustrine deposits (Fig. 4), which are naturally highly erodible. At Tuanjie, ~~T~~the ~~he thickness of~~ lacustrine deposits ~~in Tuanjie is~~are >200 m thick, and the ~~lateral~~longitudinal (stream-wise)~~–~~ lengths of the seven terraces range from 150 to 1000 m (Fig. 4, Table 2)~~.,~~ ~~Terrace T1 has the most significant extension towards the center~~ centre ~~of the Diexi Lake (Fig. 1c).~~ The Taiping terraces are developed on ~~the~~ a hillside with a slope of 40°~~–~~–60°, and is therefore influenced by landslides and some human activity~~croplands~~. The ~~horizontal extensions~~lateral extent of T1, T2, and T3 varies from 190 to 520 m (Table 2).~~are equal to 520 m, 380 m,~~

and 190 m, respectively. Correlations between the terrace levels at the two sites are given in Table 2 and Fig. 4.

Terrace elevations were obtained using the Light Detection And Ranging (LiDAR) with a 0.5 m accuracy and the Advanced Spaceborne Thermal Emission and Reflection Radiometer Global Digital Elevation Model (ASTER GDEM) with a 30 m accuracy (Fan et al., 2021). The data were imported in ArcGIS 10.3, and field investigations on two Terraces determined their altimetric level (Table. 2), textures, and formation agessedimentary sequences (Fig. 4). The elevation data reported in Fig. 1c and 1d show are the elevations of all the terrace surfaces.

Table. 2. Elevation and correlation of terraces at of the Tuanjie and Taiping. Diexi Lake currently stands at ~ 2150 masl.

Tuanjie terraces	Elevation (masl)	Width (m)	Taiping terraces	Elevation (masl)	Width (m)
Highest	2390	-	Highest	2390	-
T7	2323	226	T3	2320	190
T6	2298	-	T2	2311	380
T5	2276	378	T1	2279	520
T4	2248	186	-	-	-
T3	2215	150	-	-	-
T2	2204	360	-	-	-
T1	2178	11000	-	-	-

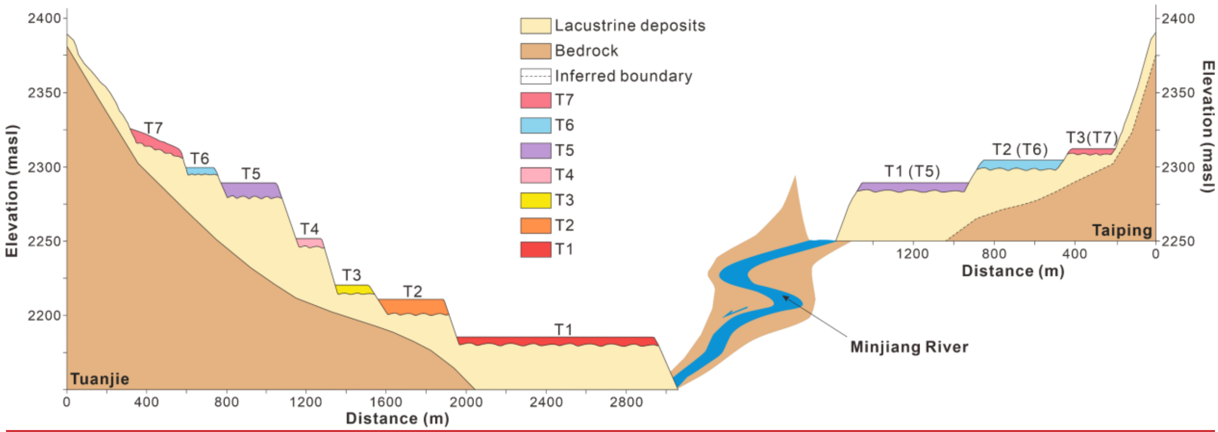

Figure 4. Sketch showing correlation between the Tuanjie and Taiping terraces (see Table 1).

4.2 Terrace~~s~~ lithostratigraphy

~~**We have summarizsed summarised the lithology, texture, and sedimentary structures of the Tuanjie and Taiping terraces.**~~

4.2.1 Tuanjie ~~Terraces~~terraces

Tuanjie terraces T1, T2, T3, T4, and T6 are characterised by a sequence of silts, sands, gravels, loess, and palaeosol units. T5 and T7 lack the loess unit (Fig. 5a) probably due to erosion via human activities, and for the same reason T4, T5, T6 and T7 show strong signs of deformation and collapse. The lithostratigraphy ~~of the Tuanjie terraces~~(Table~~.~~ 1 and Fig. 5a)~~,~~ is summarised as follows (starting from the base)~~from bottom to top, is summarized~~ summarised ~~as follows (Table. 1 and Fig. 5a)~~:

(1) Silt clay (*Fl*), ~~this unit has~~with intense weathering, horizontal bedding, and wave bedding, ~~indicating the presence of~~ ~~these are the~~ characteristic~~s~~ of lacustrine deposits~~.~~.

(2) Gravelly ~~units~~ (*Gh, Gci, Gmm*) ~~represent~~ fluvial deposits separated by an unconformity with the underlying lacustrine deposits ~~and display an unconformity with the underlying layers~~. The flow orientation of the gravels is predominantly parallel to the Minjiang River, suggesting ~~that the Minjiang River is~~it is the source of these gravels. The gravel units ~~in~~ at ~~Tuanjie~~ T1, T4, T5, and T7 (*Gh*) are generally poorly~~-~~sorted and well-rounded, with a grain-sizes ~~diameter~~ ranging ~~from~~ 2-~~ to~~ 30 cm. ~~This indicates the presence of~~Present are longitudinal bedforms, lag deposits, and sieve deposits (Fig. 5a). ~~Gravels in Tuanjie~~ At T2 (*Gci*) the gravels show inverse grading, with grain-sizes ranging~~have a~~ 2-25 cm (clasts > 35 cm are rare), ~~diameter and exhibit inverse grading. Gravels larger than 35 cm in diameter are rare, and the gravels are~~ poorly~~-ly sorted~~ sorted and sub-circular to round clasts ~~, lacking a specific direction~~ without orientation. ~~In~~ At~~Tuanjie~~ T3 (*Gci*), the gravel units exhibit inverse grading, are poorly sorted, with ~~and~~ sub-circular to round ~~gravels~~ clasts of grain-size ranging ~~with a~~ 3-25 cm~~ diameter and exhibit inverse grading~~. ~~These features suggest that the gravel units of T2 and T3 are clast-rich debris flows with high strength energy or pseudoplastic debris flows with low strength energy.~~ Gravels at~~in~~ ~~Tuanjie~~ T6 (*Gmm*) ~~have~~ show graded bedding with good sorting and rounding~~, indicating deposition by plastic debris flows with high strength energy~~.

(3) Loess (*Ls*), loess units of T1 and T2 are brick-red in colour; the ~~-~~loess at T3 contains a~~A~~ngular fragments of phyllite~~ fragments occur in T3~~.

(4) ~~Paleosol~~Palaeosols (*Ps*), if present, are ~~caps all terraces~~ ~~deposited~~developed ~~at the topmost of the~~capping the fluvial strata~~,~~, and contain ~~is characterized characterised by~~ abundant roots (Fig. 5a). L~~Above T7, are l~~acustrine deposits extend above T7 with a thickness of 30 m ~~are present~~; these deposits show~~, exhibiting~~ undulating bedding and severe denudation (Fig. 4). ~~The highest point of lacustrine deposits reaches up to 2390 m (Fig. 5a).~~

~~The strata stratigraphic sequence of each terrace exhibit variations is different. Terraces T1, T2, T3, T4, and T6 are characterizd characterised by a sequence of silts, sands, gravels, loess, and paleosol units, whereas T5 and T7 lack the loess unit (Fig. 5a). The absence of loess units in T5 and T7 may be caused bythe result of erosion and human activities. It is noteworthy that tTerraces T4 to T7 have undergone varying degrees of deformation and collapse, which. The deformation can be attributed to cultivation, excavation, and other human activity. Additionally, catastrophic eventsnatural disasters may have also contributed to the deformation. Further research is necessary to establish the precise causes of the deformation observed in these terraces.~~

4.2.2 Taiping ~~Terraces~~terraces

Taiping terraces are characterised by a sequence of lacustrine silts, muds, gravels, loess, and palaeosol units (Fig. 5b). The lithostratigraphy (Table 1 and Fig. 5b) is summarised as follows (starting from the base):

(1) Silt-clay (*Fl*) underlies all three terraces. Note that the highest extent of the lacustrine units reaches > 70 m thick.

(2) Gravelly (*Gh, Gci, Gmm*) fluvial deposits observed on the Taiping terraces all show a flow direction aligned with Luobogou Gully, indicating these gravels derive from the gully. Gravels at T1 (*Gcm*) are characterised by poorly sorted and subrounded gravels with grain-sizes of 5-10 cm. Similarly, the gravel units in T2 and T3 (*Gcm*) contain numerous broken phyllite fragments. T3 displays two beds of horizontal, angular phyllite fragments (*Gh, Gci*) with grain-sizes of 2-5 cm.

(3) Mud (*Fm*) units contain snail shells suggesting these may be overbank deposits, abandoned channels, or drape deposits. ~~and the two clast layers are composed of neatly arranged phyllite fragments (Fig. 5b).~~

(4) Loess (*Ls*) units at T2 and T3 are mixed with some angular phyllite fragments

(5) Palaeosols (*Ps*) cap all three terraces.

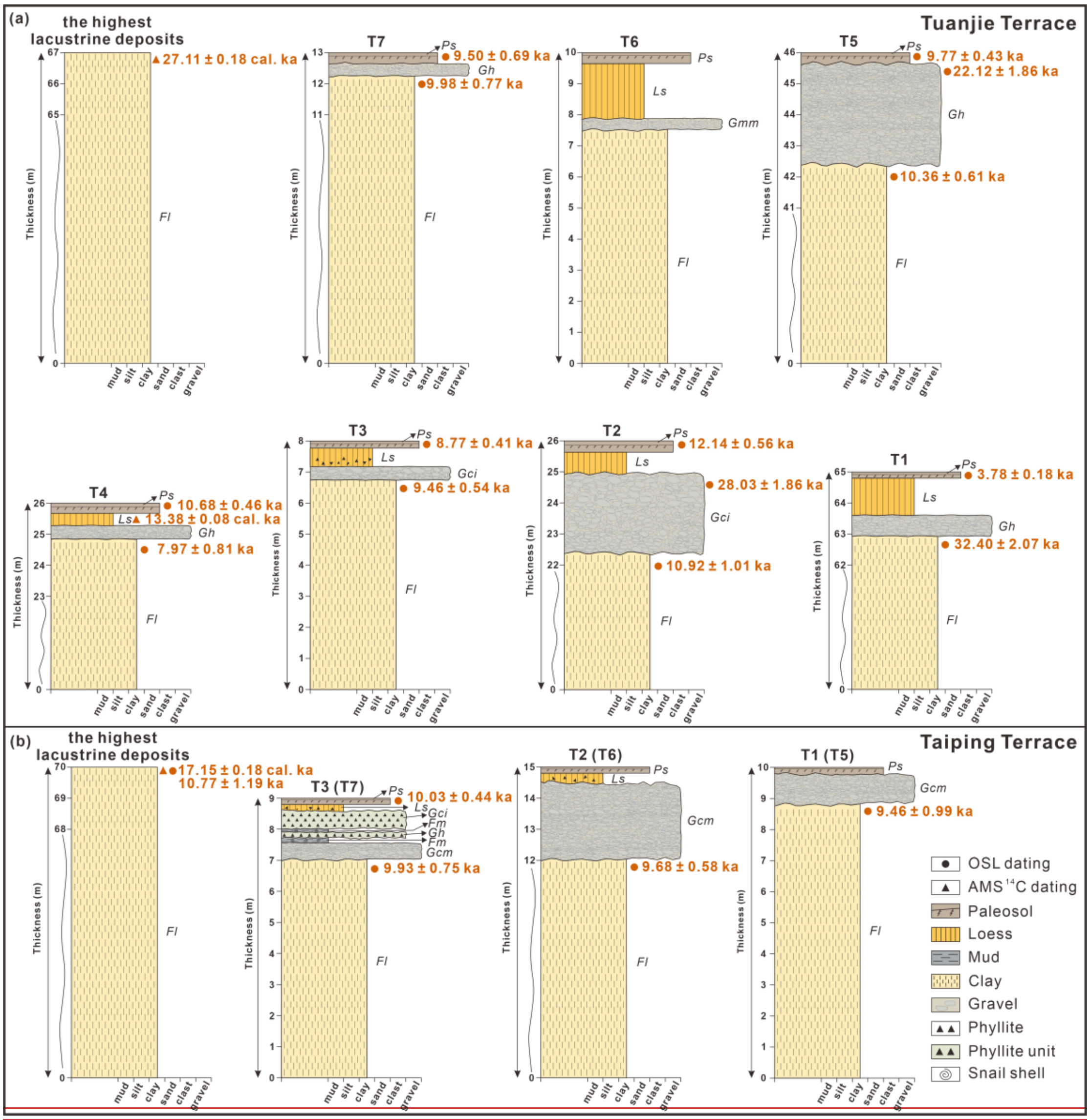

Figure 5. Terrace sedimentary sequences, lithofacies, and dating results (radiocarbon dates are denoted cal. ka): (a) Tuanjie T1, T2, T3, T4, T5, T6, T7, and the highest lacustrine deposits, respectively. (b) Taiping T1, T2, T3, and the highest lacustrine deposits. All lithofacies labels are linked to Table 1; see Table 2 and Fig. 4 for terrace correlations.

~~In Taiping, a set of~~ the bottom strata of these ~~three~~ terrace staircases ~~are~~ also has a base consisting of lacustrine deposits, as Fan et al. (2021) documented. The sedimentary sequences of Terraces T1 and T2 are comparable to T5 and T6 of the Tuanjie terracessite (Fig. 5). Taiping T1 is covered by gravels and paleosol, while T2 is ~~characterized~~ characterised by a sequence of gravels, loess and paleosol (Fig. 5b). Terrace T3, however, has different ~~features~~ sequences. It consists of a gravel unit (*Gcm*) overlying two sequences of mud (*Fm*) phyllite clasts (*Gh, Gci*) layers (Fig. 5b). The mud layers in T3 contain snail shells, and the two clast layers are composed of neatly arranged phyllite fragments (Fig. 5b).

The three gravel units observed in the Taiping terraces have a directional pattern along the Luobogou Gully, indicating their origin from a high-energy event within the gully. Gravels in Taiping T1 (*Gcm*) are characterized characterised by poorly sorted and subrounded gravels with a diameter of 5-10 cm, implying the presence of a pseudoplastic debris flow (Fig. 5). Similarly, the gravel units in Taiping T2 and T3 (*Gcm*) contain numerous broken phyllites, indicating the occurrence of pseudoplastic debris flows. The loess units in Taiping T2 and T3 (*Ls*) are mixed with 2-5 cm diameter of angular phyllites., This feature suggestssuggesting the presence of high-energy environments that facilitated the mixing of loess with phyllite clasts. Furthermore, the two mud-phyllite clasts layers in Taiping T3, indicate that two blocking events occurred downstream. The presence of snail shells within the mud layers suggests the occurrence of overbank deposits, abandoned channels, or drape deposits (Fig. 5).

4.3 OSL ages

We obtained measured 19 quartz OSL agesdates in total:, with 14 onessamples from the Tuanjie terraces and the other 5 onessamples from the Taiping terraces (summarised in Fig. 5 and , as presented in Table 3).

At Tuanjie, OSL dating ofthe depositional ages of the lacustrine deposits in Tuanjie range from ~32 ka to 10 ka and do not follow a simple elevational sequence. terraces yielded ages of 32.40±2.07 ka for the T1, 10.92±1.01 ka for the T2, 9.46±0.54 ka for the T3, 7.97±0.81 ka for the T4, 10.36±0.61 ka for the T5 and 9.98±0.77 ka for the T7. Consequently, T1 was deposited formed in the Late Pleistocene; T2, T5, and T7 were formeddeposited at the beginning of the Holocene; T3 was formeddeposited at the end of the early Holocene; and T4 was formeddeposited at the beginning of the middle Holocene. The chronological results of lacustrine deposits are chaotic. Tuanjie T1-, T2, T3, and T4 becomes display a younging trender with increasing elevation, while . Tuanjie T5 and T7 have yield similar agesa similar age, but are older than T3 and T4. The highest lacustrine deposits are only about 5 ka younger than T1. Dating results of gGravels units from the T2 and T5 yield ages show that these were deposited in the Late Pleistocene, andof the ages are 28 .03± 1.862 ka and 22.12 ± 1.862 ka, respectively. The palaeosols are all Holocene in age, mostly ages ranging from ~ 12 to 9 ka, withof the paleosol of each terrace differ, but most paleosol units were developed during the Holocene. Paleosol of T2 and T4 were deposited at the older ages of 12.14±0.56 ka and 10.68±0.46 ka, respectively. And the paleosol units of T3, T5, and T7 are deposited at 8.77±0.41 ka, 9.77±0.43 ka, and 9.50±0.69 ka, respectively. T1 yielding a notably younger has the youngest paleosol unit with an age of ~ 3.784 ka.±0.18 ka.

At Taiping, the depositional ages of all three lacustrine samples (plus the highest lacustrine sample) are consistently ~10 ka.The OSL ages of Taiping T1 to T3 lacustrine deposits are 9.46±0.99 ka, 9.68±0.58 ka, and 9.93±0.75 ka, respectively. The highest lacustrine deposits yielded an age of 10.77±1.19 ka. All the terraces were formed during the Holocene.

Table 3 Summary of OSL data.

Location	Terrace no.~~Deposit level~~	Facies	Longitude and latitude	Lab code	Quartz grain size (μm)	Sample ID	Elevation (masl)*	Sample ~~D~~depth (m)	U (ppm)	Th (ppm)	K (%)	Water content (%)	Dose rate (Gy/ka)	Dose (Gy)	Age (ka)
Taiping	-	lacustrine	32°7′37″N, 103°44′14″E	IEE5554	4-11	TP19-1	234~~32.95~~	1.90	4.82±0.14	12.85±0.37	1.98±0.03	20±5	4.27±0.14	45.93±4.84	10.77±1.19
	T3	~~paleosol~~palaeosol	32°7′34″N, 103°44′12″E	IEE5555	4-11	TP19-2	2279~~.14~~	3.50	2.92±0.05	14.75±0.20	2.01±0.02	10±5	4.28±0.15	42.95±1.10	10.03±0.44
		lacustrine		IEE5556	4-11	TP19-3		4.20	3.62±0.55	14.23±0.27	2.20±0.04	20±5	4.17±0.16	41.43±2.68	9.93±0.75
	T2	lacustrine	32°7′32″N, 103°44′11″E	IEE5557	4-11	TP19-4	22~~19.57~~20	3.60	3.29±0.10	12.59±0.40	1.90±0.01	20±5	3.71±0.12	35.89±1.80	9.68±0.58
	T1	lacustrine	32°7′33″N, 103°44′11″E	IEE5558	4-11	TP19-5	2177~~.27~~	1.00	3.31±0.07	12.74±0.19	2.17±0.02	20±5	4.02±0.13	38.05±3.78	9.46±0.99
Tuanjie	T7	~~paleosol~~palaeosol	32°2′42″N, 103°39′45″E	IEE5540	4-11	DX19-1	2315~~.45~~	2.30	3.48±0.04	13.86±0.28	2.16±0.07	10±5	4.54±0.17	43.16±2.71	9.50±0.69
		lacustrine		IEE5541	4-11	DX19-2		2.90	3.41±0.05	14.00±0.20	2.40±0.05	20±5	4.29±0.14	42.82±2.99	9.98±0.77
		~~paleosol~~palaeosol	32°2′42N, 103°39′48″E	IEE5543	4-11	DX19-4	226~~65.8~~8	1.30	2.93±0.07	13.49±0.21	2.03±0.02	10±5	4.25±0.15	41.47±1.05	9.77±0.43
	T5	fluvial	32°2′46″N, 103°39′55″E	IEE5542	90-150	DX19-3	226~~54.9~~3	2.60	2.28±0.05	10.25±0.17	1.53±0.04	10±5	2.70±0.11	59.74±4.46	22.12±1.86
		lacustrine	32°2′42″N, 103°39′48″E	IEE5544	4-11	DX19-5	226~~65.8~~8	2.80	3.14±0.05	13.34±0.13	2.16±0.05	20±5	3.96±0.13	41.03±1.98	10.36±0.61
	T4	~~paleosol~~palaeosol	32°2′40″N, 103°39′56″E	IEE5545	4-11	DX19-6	222~~8.7~~9	2.20	2.85±0.03	14.35±0.10	2.00±0.01	10±5	4.24±0.15	45.33±1.14	10.68±0.46
		lacustrine		IEE5546	4-11	DX19-7		5.00	3.57±0.06	14.13±0.36	2.45±0.04	20±5	4.34±0.15	34.59±3.33	7.97±0.81
	T3	~~paleosol~~palaeosol	32°2′40″N, 103°39′55″E	IEE5547	4-11	DX19-8	2192~~.44~~	2.20	2.99±0.29	12.78±0.19	1.96±0.07	10±5	4.11±0.16	36.05±0.91	8.77±0.41
		lacustrine		IEE5548	4-11	DX19-9		2.10	3.12±0.16	13.54±0.21	2.48±0.02	20±5	4.26±0.14	40.26±1.85	9.46±0.54
		~~paleosol~~palaeosol	32°2′46″N, 103°39′60″E	IEE5549	4-11	DX19-10	2180~~.47~~	5.00	3.40±0.05	13.97±0.23	2.41±0.06	10±5	4.70±0.18	57.06±1.52	12.14±0.56
	T2	fluvial		IEE5550	90-150	DX19-11		5.50	3.37±0.04	14.74±0.12	1.78±0.04	10±5	3.38±0.13	94.60±5.09	28.03±1.86
		lacustrine	32°2′42″N, 103°40′08″E	IEE5551	4-11	DX19-12	219~~43.8~~0	4.50	3.35±0.04	13.76±0.16	2.26±0.07	20±5	4.10±0.14	44.79±3.84	10.92±1.01

4.4 AMS ^{14}CRadiocarbon ages

Three radiocarbon ages werhe measured in total, all from bulk sediment samples (Table 4). The highest lacustrine deposits of theat Tuanjie and Taiping Terraces were depositedyielded ages of at ~ 27 .11±0.18 cal. ka BP and ~ 17 7.15±0.18 cal. ka BP, respectively. Additionally, tThe loess sample collected from Tuanjie in T4 yielded an age of of the Tuanjie Terrace was ~ deposited at 13.38±0.08 cal. ka BP. (Table 4).

Table. 4 Summary of the radiocarbon results for Tuanjie and Taiping.

Samples	Lab code	Material	Elevation (masl)	δ^{13}C (‰)	Radiocarbon age (a BP)	Calibration age (cal. ka BP)
TP-max	Beta-520926	bulk sediment	2342.95	-19.1	14050±50	17.15±0.18
TJ-max	Beta-520925	bulk sediment	2390.00	-19.2	22740±90	27.11±0.18
TJ-T4-HT	Beta-520924	bulk sediment	2280.00	-21.6	11490±40	13.38±0.08

5 Discussion

5.1 Reliability of dating results

First, we consider the reliability of our chronology. Considering Given the relatively stable depositional environment of the fine silt-rich (lacustrine and palaeosol) samples dominated nature , the relatively stable depositional environment, and the normal distribution of D_e particularly for the two coarse samples,; we assume that all they the OSL samples were well--bleached before deposition and therefore yield reliable ages..

Our ages are consistent with those reported by previous studies at Diexi, which fall mainly between about 36 and 11 ka (Table S2). We note that tAlthough the age of the the Tuanjie T1 lacustrine deposits from Tuanjie T1 (32.4 ± 2.1 ka, DX19-13, Fig. 5a) is significantly older than our other lacustrine depositsages yielded an age of 32.40±2.07 ka (32.40±2.07 ka, DX19-13, Fig. 5a); however, ,two other published sources support our result: (1) the reliability of this sample is supported by thea basalbottombasal radiocarbon age (calibrated to 35.1 ± 0.3 cal. ka BP) reported from the Diexi Lake ZK2 drill-core of the ZK2 core ((Wang et al., 2012), and (2) two radiocarbon and the upper and lower age limitsages of thefrom another lacustrine section at Tuanjie (calibrated to 35.8±0.4, and 30.7±0.03 cal. ka

BP) reported by section Zhang et al. (2009).–

Both Comparing all the dating results ages withinof the Tuanjie Tterraces, the gravel units of at Tuanjie –T2 and T5 (~ 28 and 22 ka, respectively) yield have OSL ages that are much older ages than thethe underlying lacustrine deposits (~ 11 and 10 ka, respectively) of T2 and T5, respectively (Fig. 5). In this case, we favour the lacustrine ages and exclude the samples collected from thin sand lenses within the gravels.

However, tThese two fluvial deposits have the similarity ages with the convolution structures in Haizipo (27.24±0.41 cal. ka BP, 27.74±0.47 cal. ka BP; Wang et al., 2012), suggests the reliability of the gravel ages. The gravel units in Tuanjie T2 and T5 these fluvial deposits and the convolution structures in Haizipo were formed concurrently at the same time.

At Taiping, our radiocarbon-OSL dating pair collected from tThe highest lacustrine deposits in Taiping underwent hasyields –paired radiocarbon and OSL dating, resulting in ages of 17.152 ± 0.18 2 cal. ka BP and 10.778 ± 1.19 2 ka, respectively (Fig. 5). In this case, we suspect the radiocarbon age is overestimated The discrepancy between the two dating methods reveals that the radiocarbon age appears to be approximately 6,000 years than the OSL age. This difference suggests a potential overestimation of radiocarbon ages due to the 'old carbon reservoir' effect effect. Several This reservoir effect in the sample can result from several factors, contribute to the reservoir effect, including: (1) the lower ^{14}C specific- activity carbon and the atmosphere-water exchangein the lake water and sediments compared to the atmosphere (Deevey et al., 1954). (Deevey et al., 1954; Keaveney and Reimer, 2012; Ascough et al., 2016); (2) landslides, debris flows, or other disturbances can causeing surface sediments to fall downhilldrop into the lake, , and mixing older sediments with younger onesnew subaqueous landslides, slumps, or other disturbances may have mixed older sediments with younger ones (Counts et al., 2015; Shi, 2020); and. (3) the re-deposition of older organic components, such as stored charcoal leading toresulting in a pre-dating bias in the biological indicators of sediments (Kaplan et al., 2002; Krivonogov et al., 2016).

Besides, previous studies show that the ages of the lacustrine deposits along the Diexi area are mainly between 35.78 and 10.63 ka (Table. S2). Our dating results of lacustrine deposits lie within this range, supporting our data are reliable.

5.2 Terraces along the upper Minjiang River

~~Along the upper Minjiang River, there are a~~ A m~~m~~inimum of fifteen sets of river terraces occur a~~,~~ long the upper Minjiang River valley, with nine ~~terraces~~ sets located upstream of ~~the~~ Diexi ~~area~~ (from Gonggaling to Zhangla~~Zhangla to Gonggaling~~), two sets ~~terraces~~ near ~~the~~ Diexi ~~area~~ (Taiping and Tuanjie), and four ~~terraces~~ sets ~~are developed~~ downstream (the~~from~~ Maoxian-Wenchuan area). From previously published work, we compiled a~~A~~ total of 124 dates (OSL, infra-red stimulated luminescence, thermoluminescence, radiocarbon and Electron spin resonance)~~sample~~ measured on the terraces of the upper Minjiang Rivers~~ for terrace dating were collected from these regions terraces~~ (Table~~.~~ S2)~~, including thirty-two samples from the upstream, eighty-three samples from the Diexi area, and nine samples from the downstream~~. T~~he~~ erraces ~~ages of the upstream terraces indicate that the formation and evolution of terraces~~upstream of Diexi ~~in the upper Minjiang River~~ go as far back as ~ ~~began around~~ 830 ka (Zhao et al., 1994), but fall ~~and~~ primarily ~~formed~~ between ~ 47- and 2 ka (Fig. 6). –T~~he ages of these t~~erraces~~s~~ in the Diexi area ~~have ages that are distributed~~span ~~between~~ ~ 5050 ~~and~~ to ~~50~~ 2 ka (Kirby et al., 2000; Duan et al., 2002; Yang et al., 2003; Gao and Li, 2006; Wang et al., 2007; Wang, 2009; Mao, 2011; Jiang et al., 2014; Zhong, 2017; Guo, 2018; Luo et al., 2019; Zhang, 2019; Wang et al., 2020b)~~,~~ with the majority, ~~observed~~ ~~are between~~ 32-2 ka (Fig. 6). Downstream reaches host terraces ~~were deposited formed between~~ranging ~ 400 ~~and~~ to 50 ka (Zhao et al., 1994; Yang et al., 2003; Yang, 2005; Zhu, 2014), with a significant fraction falling ~~portion terraces formed~~ between ~ 40 ~~to~~ and 20 ka (Fig. 6). ~~In summary, the terrace ages dating results along the upper Minjiang River span from 830 to 1 ka, with and the majority of terraces formed between 40 and 6 ka. The Diexi area shows a higher concentration ofhas many terraces than the upstream and downstream regions, with these terraces primarily formed from 30 to 0 ka.~~

~~The t~~Terraces upstream ~~in the area~~ ~~(stretching from the~~ Zhangla basin to the source of the Minjiang ~~River)~~ are attributed to tectonic uplift (Yang et al., 2003; Yang, 2005; Yang et al., 2008; 2011; Chen and Li, 2014; Zhu, 2014). Whereas, by contrast, the Tuanjie and Taiping terraces are thought to relate to the evolution of the Diexi palaeo-dam (Duan et al., 2002; Wang et al., 2005b; Wang, 2009; Zhu, 2014). ~~Although Diexi and Zhangla are located on the Minjiang fault, in the Diexi area, the formation and evolution of the Tuanjie and Taiping Terraces are different, they were influenced by the evolution of a palaeo-dam~~ (Duan et al., 2002; Wang et al., 2005b; Wang, 2009; Zhu, 2014)~~.~~ T~~he~~ erraces downstream

~~downstream terraces~~ in the Maoxian-Wenchuan region –share similar ~~features~~ characteristics to those at ~~with the terraces in~~ Diexi, as they are also believed to have formed ~~as a result of the~~via outburst flooding from ~~of~~ a palaeo-dammed lake (Zhu, 2014). However, ~~the~~those terraces are also strongly influenced by activity along the ~~downstream terraces are located in~~ ~~on~~ ~~the~~ Maoxian-Wenchuan fault zone~~, which makes it~~ ~~a~~ ~~different~~ ~~formation process~~ ~~from the Diexi terraces in the formation process~~. We hypothesise that ~~All these indicate that~~ the formation and evolution of the Diexi terraces (at Tuanjie and Taiping) are distinct and independent of the upstream and downstream terraces. We test and discuss this idea further i~~. I~~n the following sections.~~, we will present additional evidence to explore this phenomenon further.~~

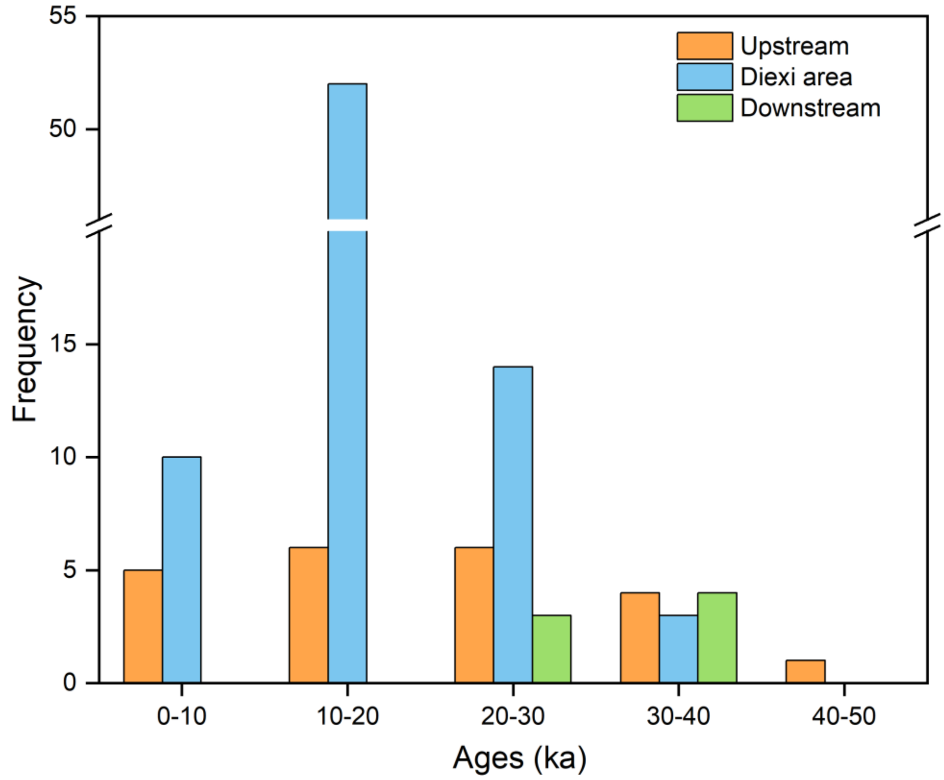

Figure 6. Frequency distribution histogram of terrace ages since 50 ka in the upper reaches of the Minjiang River (at Diexi, upstream, and downstream). By far the most frequent terrace age falls between 20 and 10 ka.

5.3 Correlation of the Tuanjie and Taiping ~~Terraces~~terraces

The highest lacustrine deposits ~~in~~ at Tuanjie and Taiping ~~have equal~~occur at the same elevation (~ 2390 masl), –suggesting that the two sets of terraces ~~Taiping Terraces and Tuanjie Terraces~~ are also related somehow ~~related~~.

The Tuanjie and Taiping terraces certainly share similar lithostratigraphy (Fig. 5). For instance, Tuanjie T5/Taiping T1 share the same sedimentary sequence (from the base to top): silty-clays (*Fl*), gravels (*Gh* at Tuanjie, *Gcm* at Taiping) and palaeosol (*Ps*), and very similar sequences are shared by Tuanjie T6/Taiping T2, and Tuanjie T7/Taiping T3. In addition, the chronology (Table 3) we have from the lacustrine deposits at Taiping T1 (9.5 ± 1 ka) and Tuanjie T5 (10.4 ± 0.6 ka) compare closely, as do Taiping T3 (10 ± 0.8 ka) and Tuanjie T7 (10 ± 0.8 ka). Based on these considerations, together with their elevation, we suggest that Taiping T1, T2, and T3 correspond to Tuanjie T5, T6 and T7 (Fig. 4).

5.4 Controls on terrace formation at Diexi: tectonism, climate or outburst floods?

The formation of terraces in mountain rivers is typically attributed to either tectonic activities (Burgette et al., 2017), climate change (Maddy et al., 2005; Gao et al., 2020), or some combination of those (Luo et al., 2019; Chen et al., 2020; Narzary et al., 2022; Ma et al., 2023). The impact of extreme events on terraces has come to the attention of researchers more recently (Hewitt, 2016; Wang et al., 2021a; Yu et al., 2021). At Diexi, the great thickness (> 200 m) of lacustrine deposits carved by floodwaters and topped discontinuously by terrace gravels and loess-palaeosol sequences, suggests a role for tectonism, climate, and outburst floods, but the relative influence of each is yet to be clarified. We pursue this question below.

~~Other evidence comes from the characteristics of sedimentary stratigraphy, thus the T1 to T3 terraces of Taiping correspond to the T5 to T7 terraces of Tuanjie (Fig. 4). Terrace T5 (Tuanjie) and T1 (Taiping) have the same sedimentary sequences from the bottom to the top, including clays (*Fl*), gravel unit (*Gh* in Tuanjie, *Gcm* in Taiping) and paleosol (*Ps*) (Fig. 5a and 5b). Paleosol (*Ps*) in T5 (Tuanjie) and T1 (Taiping) are 0.4 m and 0.2 m thick, respectively. Both T6 (Tuanjie) and T2 (Taiping) have the sequences of clays (*Fl*), gravel unit (*Gmm* in Tuanjie, *Gcm* in Taiping), loess (*Ls*), and paleosol (*Ps*). The sedimentary successions of Terrace T7 (Tuanjie) and T3 (Taiping) are both clays (*Fl*), gravel unit (*Gh* in Tuanjie, while *Gcm* in Taiping), and paleosol (*Ps*). T3 of Taiping has two sets of mud-phyllite clasts (*Fm-Gh* and *Fm-Gci*) overlaying the gravel unit (*Gcm*), and loess (*Ls*) contains phyllites. Regional geomorphic environments cause these different lithofacies and sequences.~~

~~Ages of the lacustrine deposits of Taiping T1 (9.46±0.99 ka) and Tuanjie T5 (10.36±0.61 ka), as well as Taiping T3 (9.93±0.75 ka) and Tuanjie T7 (9.98±0.77 ka) (Table. 3), are similar, which confirms from a chronological perspective that the two terraces correspond to each other (Fig. 5).~~

5.4 Formation and outburst of palaeo-dam

The triangle formed by Tuanjie and the localities of Jiaochang and Xiaohaizi lies around the center of the ancient dammed lake. Outburst sediments are present deposited downstream around the location of Xiaoguanzi-Manaoding (Fig. 1b). Combined with the lithofacies and chronological framework results in the Tuanjie terraces, the palaeo-dam has experienced multiple events of damming and dam-breaking events. We used the ages of lacustrine deposits, combined with theours and previous dating results, to classify the blocking and outburst phases of the palaeo-dam.

The palaeo-landslide dam blocked the river before 32.40±2.07 ka (Phase I, 32 ka), as supported by Wang et al. (2012) and Wang et al. (2017): (1) The bottom lacustrine deposits of the palaeo-dammed lake were deposited at 35.13±0.29 cal. ka BP. (2) In Xiaoguanzi, lacustrine deposits are overlying the accumulation deposits of palaeo-dam. The lacustrine deposits were deposited at 34.87±0.76 and 35.54±0.83 cal. ka BP. The dating results of the boundary of palaeo-lake and palaeo-dam in Xiaoguanzi supported the palaeo-lake was formed in 34.87±0.76 and 35.54±0.83 cal. ka BP. (3) Accumulation deposits of a palaeo-dam in Manaoding were deposited at 34.54±0.16 cal. ka BP.

After the first dammed lake phase, the first outburst occurred at 27.11±0.18 ka (Phase II, 27 ka), as evidenced by the deposition of outburst sediments downstream that deposited at 27.30±2.80 ka (Ma et al., 2018). Additionally, the presence of deformed layers in the Shawan section (26.5-24.1 ka; Wang et al., 2011; Wang et al., 2012), and the convolution structure in Haizipo (27.74±0.47 ka; Wang et al., 2012), confirm that a catastrophic event occurred around 27.11±0.18 ka. Furthermore, the discovery of the palaeo-landslide in Qiangyangqiao (26.54±0.53 ka, 27.28±0.41 ka; Wang et al., 2012), and the palaeo-dammed lake in Maoxian (26.81±0.98 ka; Wang et al., 2007), suggests that the upper reaches of the Minjiang River experienced several disastrous extreme events around 27 ka.

Subsequently, the palaeo-dam blocked the river again (Phase III, during 27~17 ka), and the lake level may have reached or exceeded the position of the highest lacustrine deposits in the Taiping Terrace. Around 17 ka, the palaeo-dam was broken (Phase IV, 17 ka), exposing the highest lacustrine deposits of the Taiping Terraces were exposed. Besides, the palaeo-landslide in Manaoding occurred deposited at 16.75±0.62 cal. ka BP (Wang et al., 2012), suggesting that the second outburst event happened around 17 ka.

As seen from our dating results, the lake level of the palaeo-lake descended from the highest point at the Taiping site to the T1 terrace at the Taiping between 10.77±1.19 and 9.46±0.99 ka. Furthermore, between 10.36±0.61 and 9.98±0.77 and 10.36±0.61 ka, the lake level descended from the position of T7 to T5 in the Tuanjie Terrace. These findings indicate significant lake level fluctuations in the lake level of the palaeo-dammed lake at around 10 ka, suggesting there was a third dam outburst eventduring this period (Phase V, ~10 ka). The third outburst event can be attributed to a progressive failure of the palaeo-dam. Additionally, the fluctuation in the lake level of the palaeo-lake at around 10 ka is also evident appeared in the Taiping, Shawan, and Tuanjie profiles (Zhong, 2017). Subsequently, the dam body stabilized until the occurrence of the fourth dam break event happened around 9 ka (Phase VI), leading to the formation of the present riverbed.

About 30 ka BP, during the last glacial period, the formation of Tuanjie Terrace may have been influenced by tectonic activities (such as earthquakes) and climate changes (Wang, 2009; Wang et al., 2012; Shen, 2014; Luo et al., 2019). To better understand the constraints of tectonic activities, climate changes, and the evolution of the palaeo-dam on terrace formation, we discuss the effects of these three factors below.

5.5 The formation and evolution mechanisms of the terraces

Numerous studies stated that tectonic activities and climate changes play essential roles in the generation of mountainous terraces and landscape evolution (Maddy et al., 2005; Burgette et al., 2017; Chen et al., 2020; Gao et al., 2020; Narzary et al., 2022; Ma et al., 2023). More recently, researchers have also considered the impact of extremedisaster events (Hewitt, 2016; Wang et al., 2021a; Yu et al., 2021). In the Diexi area, the substantial huge thickness (>200 m) of lacustrine deposits and the multiple loess-paleosol sequences, suggest that tectonic uplift, climate fluctuations, and the effects of damming event influence terraces. Moreover, about 30 ka BP, during the last glacial period, the evolution of Tuanjie Terrace may have been influenced by tectonic activities (such as earthquakes) and climate changes (Wang, 2009; Wang et al., 2012; Shen, 2014; Luo et al., 2019). Here, we discuss the impact of these three factors on the Tuanjie and Taiping terraces.

5.~~5~~4.1 ~~The reflection of terraces to~~Effects of tectonism on the Diexi terraces~~e activities~~

The Tuanjie and Taping terrace sites are sufficiently close (12 km) to be considered subject to the equivalent ~~Considering the short distance of only 12 km between Tuanjie and Taiping, we regard them as in the same~~ tectonic ~~uplift~~forcing~~ing background~~. In Section 5.2, we divided the upper Minjiang River into three ~~parts~~segments: Gonggaling to ~~-the~~ Zhangl~~a~~a ~~to Gonggaling area~~ (upstream of ~~the~~ Diexi ~~area~~), the Diexi area ~~(Taiping-Tuanjie)~~, and the Maoxian-Wenchuan area (downstream of ~~the~~ Diexi ~~area~~). Since the initial damming at the Diexi palaeo-landslide, ~~During the damming period of the Diexi palaeo-dammed lake (32-10 ka),~~ the fluvial incision rates in these three ~~sections~~ segments of the upper Minjiang ~~ranged fro~~is measured at~~m~~ 8.3–~~-~~85.3 mm/yr, 13.6–~~-~~198 mm/yr, and 58 mm/yr, respectively~~, from upstream to downstream~~ (see Table~~.~~ S2). In comparison, t~~T~~he Minshan Block ~~(,~~which includes the reach from Gonggaling to Maoxian~~the Minjiang River~~)~~,~~ ~~has~~ is thought to have experienced an average uplift rate of 1.5 mm/yr ~~since~~ during the Quaternary (Zhou et al., 2000). Clearly, recent incision rates in the Diexi area have been several-times faster than the average uplift rate of the Minshan Block. This highlights the unique character of Diexi and suggests that tectonic activity is not a primary factor in the formation of the terraces.

~~It can be observed that the incision rates of the upper reaches of the Minjiang River during the period of 32-10 ka are significantly higher than the uplift rate of the Minshan Block, indicating that tectonic activity has little influence on the formation of regional terraces. In particular, the Taiping-Tuanjie region has a higher incision rate than the upstream and downstream areas, highlighting its unique characteristics. Thus, tectonic activity is not a critical primary factor in the evolution of Tuanjie and Taiping terraces during 32-9 ka.~~

5.~~5~~4.2 Effects of climate changes on the Diexi terraces~~Climate fluctuations affected the formation of terraces~~

The regional climate ~~Diexi~~ has undergone three transitions from cold~~ and~~-dry to warm-~~ and~~ humid climates ~~during~~ between ~ 40 and ~~.5~~ 30~~.0~~ ka (Zhang et al., 2009) followed by~~. Later on, during the period of 30-10 ka, Diexi experienced more than~~more than ten ~~ten~~ distinguishable climatic and environmental ~~stages,~~ alternati~~ng~~ons of ~~between~~ cold ~~and~~ to warm ~~during~~between 30 and -10 ka (Wang, 2009; Wang et al., 2014). ~~In the Zhangla Basin, the climate was cold from 35 to 20 ka, but it changed from~~while it was cold to warm during 20-10 ka (Zhu, 2014). Tuanjie area had a similar climate trend to the Zhangla Basin during 20-10 ka, and Diexi has been subject to frequent climate fluctuations since 40 ka.

The chronological results ofThe the terraces at Tuanjie and Taiping span the past 32 ka, so to investigate the influence of climate we terraces range from 32.40±2.07 ka to 3.78±0.18 ka. We compared our dating agesresults withexamine the the climate variations over the same period – in the climate curves (Fig. 7). – Curves a, b, c, and d respectively represent the δ^{18}O of the Sanbao Cave, the Hulu Cave, the East Asian Monsoon, and the GISP 2 δ^{18}O record. These four climate proxies revealcurves show significant fluctuations from the end of the Last Glacial Maximum (LGM) to the early Holocene, followed by an abrupt change upon entering in therelative stability throughout the Holocene.

It is tempting to speculate that warmer periods triggered wetter conditions or glacier melt leading to the overtopping of the palaeo-dam and formation of terraces; however, –we cannot see any clear relationship between the age of the terraces and the climatic variations over the past 35,000 yrs (Fig. 7). Nevertheless, two important points are worth making:

(1)

However, cClimateA fluctuating climate change – can affectmay be seen in the topography shape of the terraced staircaseslandscape geometry. In papers by Mao (2011)-, Jiang et al. (2014)-, and Shi (2020), it is argued that -Tuanjie Terrace T2 has displays an irregular sequence of ages with age depth sequence, indicatingthat suggest repeated fluctuations in the lake level by up to 11 meters during the period ofbetween 18.60±2.8619~ and 10.63±1.2711 ka (Table. S2). Regarding Tuanjie T1, we note the extraordinary terrace width. Following the model described by Malatesta et al. (2021)Malatesta et al. (2021), we suggest that (!!! INVALID CITATION !!! (ages dated by Mao, 2011; Jiang et al., 2014; Shi, 2020)). This suggests that the geomorphological features of Tuanjie Terraces T1 and T2 have been influenced by climate change. The repetitive long-term wave erosion associated with, the fluctuating along lake shoreline the shore of the palaeo-lake beach, resulted in the bevelling and back-wearing atof T2 T1, creating a very wide terrace (Fig. 8). We note some additional erosion may have occurred owing to the positioning of the Tuanjie terraces on the concave margin of the valley (Fig. 1b) where lateral fluvial erosion tends to be accentuated. (Malatesta et al., 2021). However, it should be noted that the beveling and backwearing are not primarily affected by the repeatedly dropping and rising of the lake level. Tuanjie terraces are located at the bend of the Minjiang River, and these terraces are on the concave bank (Fig. 1b). combined with the characteristics of ""the concave bank is dominated by erosion, the convex bank is dominated by accumulation”" (Gutiérrez and Gutiérrez, 2016), supported that lateral erosion is the main factor. As a result, Tuanjie T1 has the widest terrace surface (Fig. 8).

(2) Some degree of climate control can be recognised in terms of the aeolian and weathering processes. The loess unit at Tuanjie T4 (~13.4 ± 0.1 cal. ka BP) dates to just before the Younger Dryas reflecting a cool depositional environment; loess observed at Tuanjie T3 and T2, as well as Taiping T3 and T2 suggest ages slightly younger. Most of the palaeosol units relate to the warming conditions of the early Holocene.

(3) The three outburst floods (~ 27 ka, ~ 17 ka and ~ 12 ka, reported in Section 5.5) in Diexi area were happened at the climate fluctuation periods. We speculated these floods may be the result of the glacial melting. As Wang et al. (2012) mentioned that during the Last Glacial Period, the melting of glaciers triggered massive hillslopes instability, and formed palaeo-dammed lakes.

(4) The absent of outburst flood in the Holocene may be related to the warm and stable climate.5.5.3 The instability of the palaeo-dam

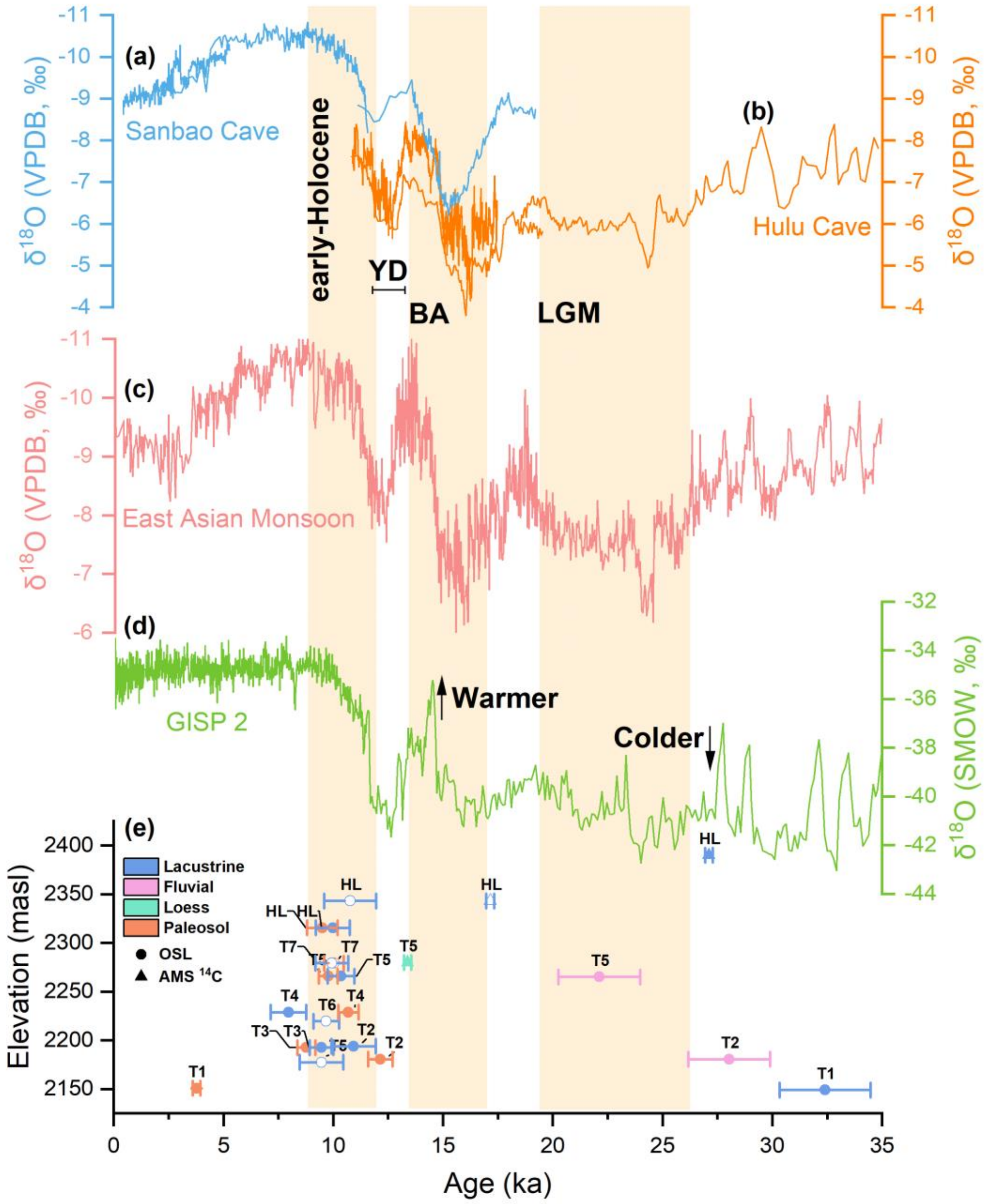

Figure 7. Palaeoclimate ($\delta^{18}O$) proxies compared with the OSL and radiocarbon chronologies obtained from the Diexi terraces. (a) Sanbao Cave (Wang et al., 2008); (b) Hulu Cave (Wang et al., 2001); (c) East Asian Monsoon (Cheng et al., 2016); (d) GISP-2 (Grootes et al., 1993); and (e) the Diexi terraces at Tuanjie (solid symbol) and Taiping (hollow symbol). The early Holocene, Younger Dryas (YD), Bølling-Allerød interstadial (BA), and the Last Glacial Maximum (LGM) are labelled.

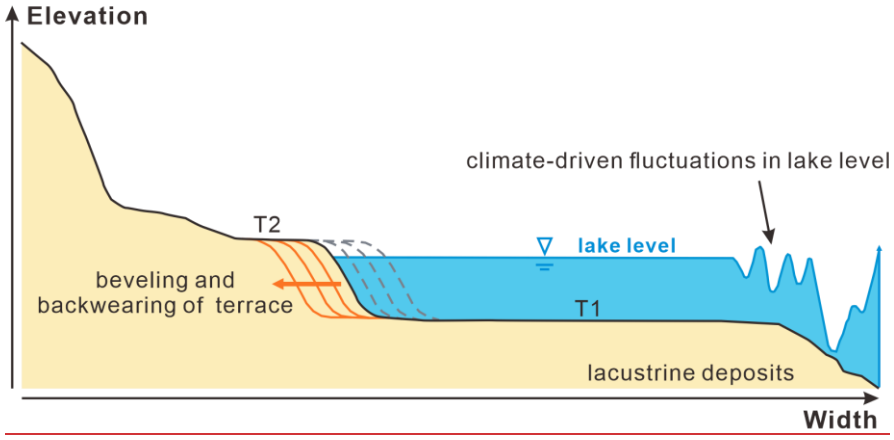

Figure 8. A schematic model showing how lake-level fluctuations drive the evolution of T1 and T2 at Tuanjie (modified from Malatesta et al., 2021). Climate-driven fluctuations in lake level result in bevelling and back-wearing of the terrace and production of the widest surface at T1.~~Damming and outburst events can strongly impact upstream and downstream areas, causing aggradation and incision (Fig. 9) (Hewitt et al., 2008; Korup and Montgomery, 2008). The upstream and downstream effects of the blockage are a rapid rise in water level resulting in the potential upstream flooding (Guo et al., 2016). The upstream sediment accumulation can abrade and protect the channel bedrock, significantly affecting river evolution and regional landscapes (Korup et al., 2010; Yu et al., 2021). During the blockage period, the dam impedes the river and maintains its base level. Gravity and density cause the material to be deposited in the Diexi palaeo-dammed lake, which erodes to form a channel. During the outburst period, the lake level drops, and the river cuts through the lake sediments, forming terraces along the river. Each outburst event does not result in a complete breach of the palaeo-dam, so the river channel cuts down through the terraces after each breach (Wang et al., 2012). Subsequently, the downstream channel restarts, forming a new, narrow, steep valley (Wang et al., 2021a).~~

5.5 Terrace formation and the evolution of the Diexi palaeo-landslide dam

Damming and outburst floods can strongly impact upstream and downstream areas, causing aggradation and incision (Fig. 9) (Hewitt et al., 2008; Korup and Montgomery, 2008). A lake formed by the blockage of a river can raise water levels upstream, resulting in the potential upstream flooding (Guo et al., 2016), and following an outburst flood, the lake level drops as a result of sudden erosion at the crest of the dam. During this lower lake level, the river cuts through the easily eroded lacustrine deposits, forming terraces.

The triangle formed by Tuanjie, Jiaochang and Xiaohaizi (Fig. 1b) marks the centre of the palaeo-dammed Diexi Lake. We suggest that this ancient lake has experienced multiple damming and breach events leading to major outburst floods down the Minjiang River. For instance, high magnitude outburst sediments are identified downstream around the Xiaoguanzi-Manaoding (Fig. 1b). Based on our terrace lithofacies and chronological analyses, we attempt to reconstruct the history of river blocking and outburst floods sourced from the Diexi Lake, as follows.

The Minjiang River was blocked by the Diexi palaeo-landslide sometime before 35 ka (Phase I: > 35 ka), as indicated by three lines of evidence: (1) the basal radiocarbon age in a drill-core from Diexi Lake is 35.1 ± 0.3 cal. ka BP ((Wang et al., 2012) (note the lacustrine pile extends ~ 80 m deeper); (2) at Xiaoguanzi, lacustrine sediments dated to 34.9 ± 0.8 and 35.6 ± 0.8 cal. ka BP ((Wang et al., 2012) are observed capping part of the palaeo-landslide dam; and (3) the same occurs at Manaoding dated to 34.5 ± 0.2 cal. ka BP ((Wang et al., 2012).

After being initially blocked by the palaeo-landslide, Diexi Lake reached its highest level around 27 ka (highest lacustrine sediments at Tuanjie date to 27.1 ± 0.2 ka, Fig. 5a). This matches the timing of evidence of the first known outburst flood (Phase II: ~ 27 ka), a gravelly unit near Xiaoguanzi (Fig. 1b), OSL-dated by Ma et al. (2018)Ma et al. (2018) at 27.3 ± 2.8 ka. Further evidence of an outburst flood (or floods) around 27 ka is indicated by two other nearby sites dated with OSL and radiocarbon, respectively: (1) a 35 m-thick sequence of deformed lacustrine bedding at Shawan (Wang et al., 2011; Wang et al., 2012) (Wang et al., 2011; Wang et al., 2012), and (2) convolution structures exposed near Jiaochang (Fig. 1b) (Wang et al., 2012). Around ~27 ka appears to have been a time of major perturbation in the upper Minjiang River: a palaeo-landslide at Qiangyang (Fig. 1b) is radiocarbon-dated to 26.5 ± 0.5 ka, 27.3 ± 0.4 cal. ka BP (Wang et al., 2012); and downstream, a palaeo-dammed lake at Maoxian is radiocarbon-dated to 26.8 ± 1.0 cal. ka BP (Wang et al., 2007).

The Diexi palaeo-dam was re-established and sedimentation in the lake resumed for about 10,000 yrs (Phase III: ~ 27–17 ka), as indicated by the highest lacustrine sediments at Taiping dated to 17.2 ± 0.2 cal. ka BP (Fig. 5b).

The second outburst flood (or floods) occurred ~ 17 ka (Phase IV). This event incised the palaeo-dam, causing the Diexi Lake level to drop by ~ 110 m (to 2279 masl), as recorded at Taiping T1 and Tuanjie T5 (Fig. 5a, b). The lowering of the lake level exposed the highest lacustrine deposits at Taiping. The palaeo-landslide at Manaoding, dated to 16.8 ± 0.6 cal. ka BP (Wang et al., 2012), is possibly linked to this second outburst flood.

In the 5000 yrs that followed (Phase V: ~ 17–12 ka), two more outburst floods may have lowered the palaeo-dam further (forming Tuanjie T4 and T3), although the timing is uncertain. Yet, we can say with confidence that an outburst flood ~ 12 ka (Phase VI), lowered the palaeo-dam by ~ 70 m (to 2204 masl), forming Tuanjie T2. From ~ 12 ka to the present (Phase VII), it appears the Diexi palaeo-dam crest has gradually incised to its current level ~ 2150 masl ~~(aside from the brief period at a higher level following the 1933 Diexi earthquake, Dai et al., 2021)~~(aside from the brief period at a higher level following the 1933 Diexi earthquake, Dai et al., 2021).–

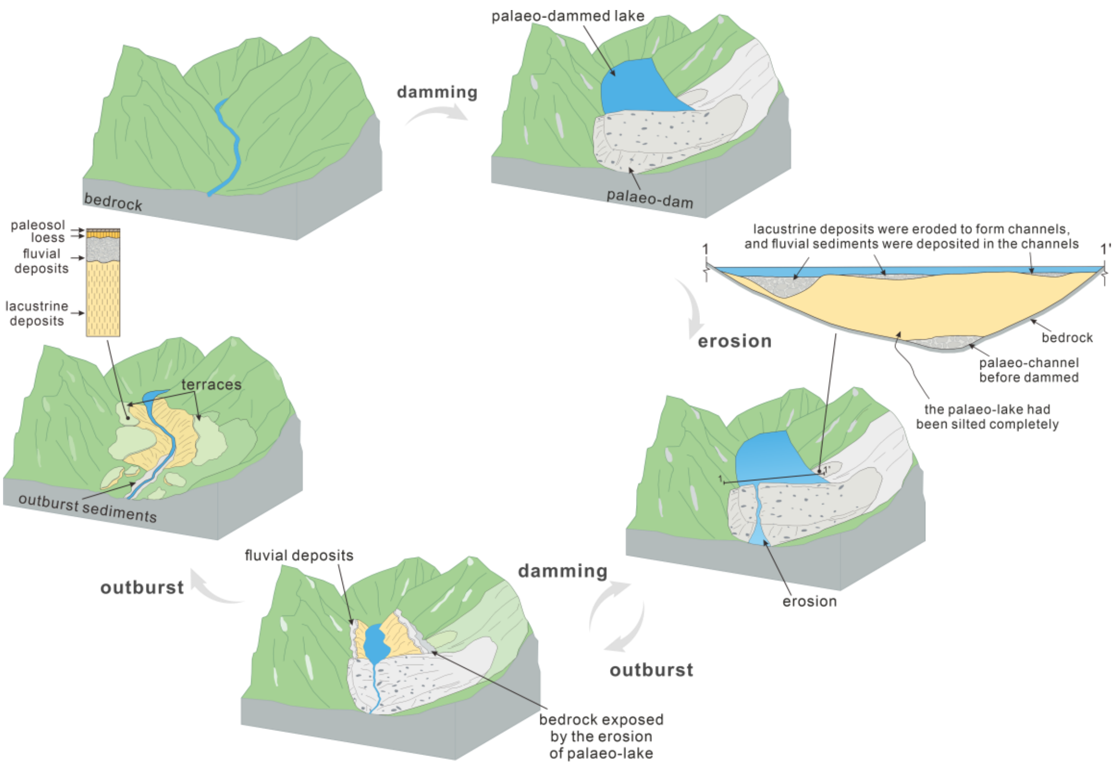

Figure 9. Model of palaeo-landslide dam evolution through time, starting with a blocking event (e.g., a major landslide), which then becomes a natural dam on the river causing a lake to form. Lacustrine deposits accumulate behind the dam, sometimes to great depth (at Diexi lacustrine sediments are > 200 m-thick). A positive water balance in the lake triggers overtopping of the dam, causing potentially catastrophic outburst floods downstream. The outburst flood typically erodes the crest of the dam subsequently lowering the lake level and allowing fluvial processes to resume along parts of the valley. This repeated process yields a terrace stratigraphy comprising (from base to top): lacustrine deposits topped by fluvial deposits perhaps capped by loess and palaeosol development.

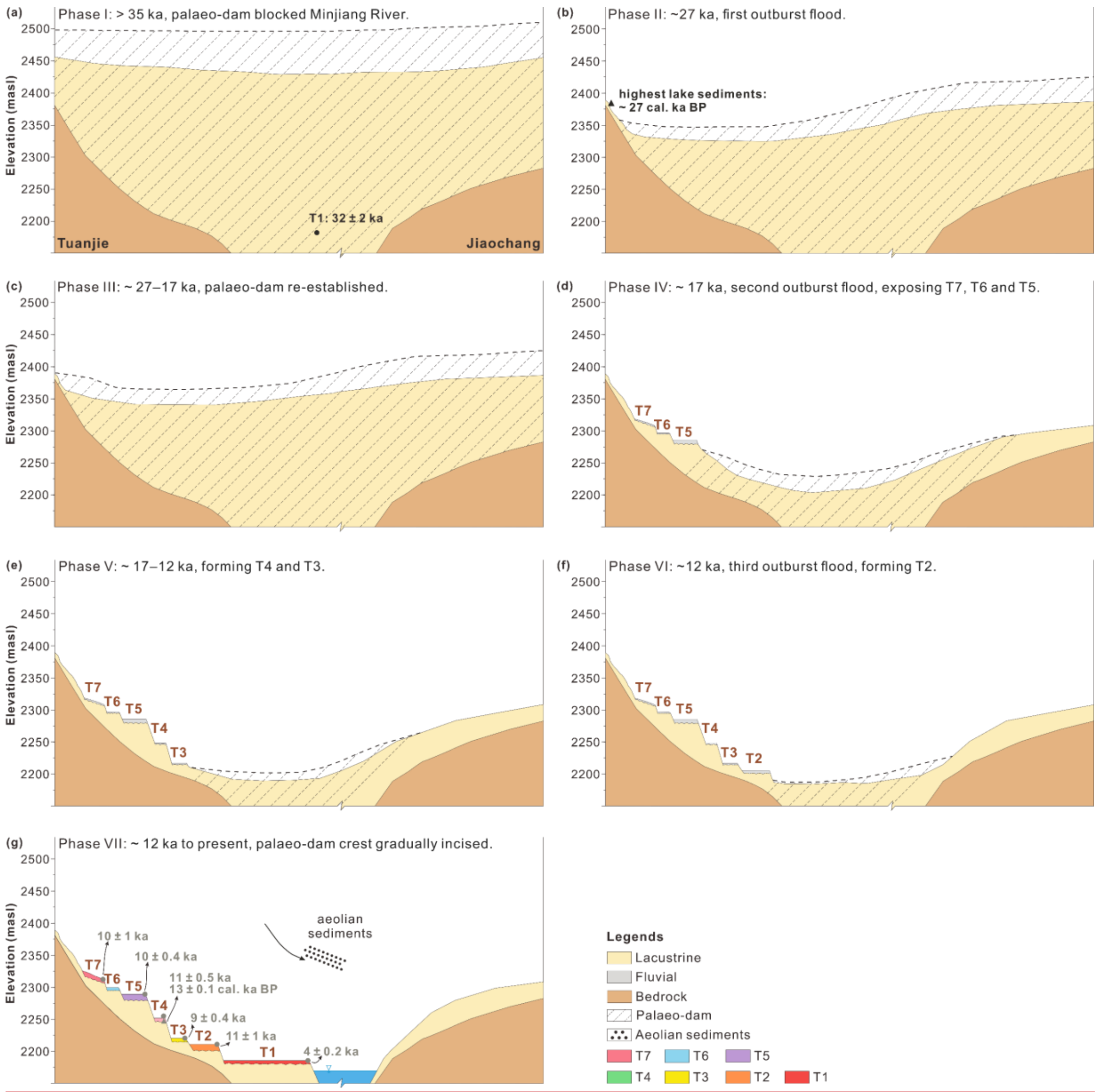

Figure 10. Schematic model of the evolution of the Diexi palaeo-dam and Tuanjie terraces. See Section 5.5 for detailed descriptions of each phase. Brown text denotes the ages of loess and palaeosol units.

6 Conclusions

We set out to investigate the origin and chronology of two sets of outstanding terraces formed upstream of the giant river-blocking Diexi palaeo-landslide on the upper Minjiang River, eastern Tibetan Plateau.

The Tuanjie terraces have seven levels (T1-T7), while those at Taiping have three (T1-T3). All terraces display a consistent sedimentary sequence comprising thick lacustrine muds topped by fluvial gravels, which at a few sites are capped by~~with~~ loess and a~~a loess-rich~~ palaeosol. We correlate T5, T6 and T7 at Tuanjie with T1, T2 and T3 at Taiping.

Our reconstruction of the history of terrace formation suggests two damming and three outburst events have occurred at the Diexi palaeo-landslide over the past 35,000 years. The sequence of events is summarised as follows: a giant landslide (>300 m high) blocked the river before 35 ka followed by the first outburst flood at ~ 27 ka; the river was blocked again between 27 to 17 ka followed by a second outburst at ~17 ka; and a third outburst at ~12 ka was followed by gradual fluvial incision of the palaeo-dam crest to its current level.

Our findings at Diexi provide a detailed case study of terrace formation coupledlinked to the evolution of the palaeo-landslide dam. The Diexi terraces (at Tuanjie and Taiping) are distinct and independent of the upstream and downstream terraces along the upper Minjiang River—they are not directly the product of either tectonic or climate forcing. Instead, terrace height and geometry are the result of the sequence of outburst floods that progressively lowered the crest of the palaeo-landslide dam (the local base level to the terraces) since its emplacement more than 35,000 years ago.

The Tuanjie and Taiping Terraces have a similar stratigraphic sequence, characterized characterised by a base of lacustrine deposits, overlain by gravels, loess, and paleosol, from the bottom to the top. The Minjiang River has transported the gravels of the Tuanjie terraces, whereas the Luobogou Gully influences the gravel in the Taiping terraces. Two sequences of mud-clast layers in the Taiping T3 terrace imply that damming events control the formation of the T3 terrace.

Combining geomorphology, sedimentology, and chronology reveals that Taiping terraces T1 to T3 correspond to Tuanjie T5 to T7. Tectonic movements and climate fluctuations are not the primary factors influencing terrace formation and evolution; instead, damming and outburst events play a crucial role. Two damming and four outburst events have been identified. Before 32 ka, the river was blocked, causing the lake level to rise rose to its highest recorded level based on lacustrine deposits. The dam remained intact until 27 ka, when the first outburst event happened. During this event, the height of the palaeo-dam dropped to near the surface of Tuanjie T2. The palaeo-dam blocked the river again between 27 and 17 ka, allowing and the lake surface to extend toward the Taiping Terracevillage. Another outburst event occurred around 17 ka, exposing the highest lacustrine deposits were exposed. The formation of the Tuanjie T7 to T5 corresponds to the third dam-breaking period, which occurred approximately 10 ka ago as a progressive outburst event. The formation of the Tuanjie T4, T3, and T1 are associated with the fourth progressive collapse event around 9 ka.

~~This finding has important implications for revealing the formation and evolution of the Diexi palaeo-landslide dammed lake. It provides crucial knowledge that contributes to understanding the formation and evolution of these terraces and reconstructing the evolution of the Diexi palaeo-landslide dam.~~ This study proposes a new perspective on terrace formation ~~in the eastern margin of the Tibetan Plateau, which~~ in ~~the~~ steep rivers draining landslide-dominated mountain belts. Given the frequent observation of valley blocking dams in high mountain settings, we suspect that the terrace formation processes described here may be more widespread than has been previously recognised.

~~can enhance our understanding of the impact of landslide dams on fluvial evolution. Additionally, it holds important implications in studying the evolution of palaeo-climate and palaeo-environment, providing insight into future mountainous engineering projects.~~

Author contributions

JL wrote the manuscript and ~~analyzed~~ analysed the data; ~~.~~ XF and ZD discussed the results and provided guidance and funding; JDJ reframed ~~some~~ data interpretations and revised the text comprehensively following review; ~~.~~ SK conducted the OSL dating; and ~~,~~ ML polished the language.

Competing interests

An author is a member of the editorial board of the journal, Earth Surface Dynamics. The peer-review process was guided by an independent editor, and the authors have ~~also~~ no other competing interest to declare.

Acknowledgments

We thank Lanxin Dai, Chengbin Zou, Yujin Zhong, Binbin Luo, Bing Xia, Kunyong Xiong for fieldwork assistance, and Xiangyang Dou for revising the figures.

Financial support

This research is financially supported by the Funds for National Science Foundation for Outstanding Young Scholars, Grant no. 42125702, the National Natural Science Foundation of China, Grant no. 42207223, the Natural Science Foundation of Sichuan Province, Grant no. 2022NSFSC003, and the State

Key Laboratory of Geohazard Prevention and Geoenvironment Protection Independent Research Project, Grant no. SKLGP2021Z025.

References

An, W., Zhao, J., Yan, X., Li, Z., and Su, Z.: Tectonic deformation of lacustrine sediments in qiangyang on the Minjiang fault zone and ancient earthquake, Seismology and Geology, 30, 980-988, https://doi.org/10.3969/j.issn.0253-4967.2008.04.014, 2008.

Arzhannikov, S., Arzhannikova, A., Ivanov, A., Demonterova, E., Yakhnenko, A., Gorovoy, V., and Jansen, J.: Lake Baikal highstand during MIS 3 recorded by palaeo-shorelines on Bolshoi Ushkanii Island, Boreas, 50, 101-113, https://doi.org/10.1111/bor.12464, 2020.

Arzhannikov, S. G., Ivanov, A. V., Arzhannikova, A. V., Demonterova, E. I., Jansen, J. D., Preusser, F., Kamenetsky, V. S., and Kamenetsky, M. B.: Catastrophic events in the Quaternary outflow history of Lake Baikal, Earth-Science Reviews, 177, 76-113, https://doi.org/10.1016/j.earscirev.2017.11.011, 2018.

Ascough, P. L., Cook, G. T., Church, M. J., Dunbar, E., Einarsson, Á., McGovern, T. H., Dugmore, A. J., Perdikaris, S., Hastie, H., Friðriksson, A., and Gestsdóttir, H.: Temporal and Spatial Variations in Freshwater14C Reservoir Effects: Lake Mývatn, Northern Iceland, Radiocarbon, 52, 1098-1112, https://doi.org/10.1017/s003382220004618x, 2016.

Avsin, N., Vandenberghe, J., van Balen, R., Kiyak, N. G., and Ozturk, T.: Tectonic and climatic controls on Quaternary fluvial processes and river terrace formation in a Mediterranean setting, the Goksu River, southern Turkey, Quaternary Research, 91, 533-547, https://doi.org/10.1017/qua.2018.129, 2019.

Bell, C. M.: Punctuated drainage of an ice-dammed quaternary lake in southern South America, Geogr Ann A, 90a, 1-17, https://doi.org/10.1111/j.1468-0459.2008.00330.x, 2008.

Burgette, R. J., Weldon, R. J., Abdrakhmatov, K. Y., Ormukov, C., Owen, L. A., and Thompson, S. C.: Timing and process of river and lake terrace formation in the Kyrgyz Tien Shan, Quaternary Science Reviews, 159, 15-34, https://10.1016/j.quascirev.2017.01.003, 2017.

Caputo, R., Salviulo, L., and Bianca, M.: Late Quaternary activity of the Scorciabuoi Fault (southern Italy) as inferred from morphotectonic investigations and numerical modeling, Tectonics, 27, 1-18, https://doi.org/10.1029/2007tc002203, 2008.

Chen, G., Zheng, W., Xiong, J., Zhang, P., Li, Z., Yu, J., Li, X., Wang, Y., and Zhang, Y.: Late Quaternary fluvial landform evolution and controlling factors along the Yulin River on the Northern Tibetan Plateau, Geomorphology, 363, https://doi.org/10.1016/j.geomorph.2020.107213, 2020.

Chen, H. and Li, Y.: River terrace responding to the obduction of the Longmenshan fault zone in the upper Min River basin, Mountain Research, 32, 535-540, https://doi.org/10.16089/j.cnki.1008-2786.2014.05.003, 2014.

Chen, Y., Aitchison, J. C., Zong, Y., and Li, S.-H.: OSL dating of past lake levels for a large dammed lake in southern Tibet and determination of possible controls on lake evolution, Earth Surface Processes and Landforms, 41, 1467-1476, https://10.1002/esp.3907, 2016.

Chen, Z. and Lin, Q.: Significance of neotectonic movement of lake extension and shrinkage in Qinghai-Tibet Plateau, Earthquake, 31-40+52, https://doi.org/CNKI:SUN:DIZN.0.1993-01-006, 1993.

Cheng, H., Edwards, R. L., Sinha, A., Spötl, C., Yi, L., Chen, S., Kelly, M., Kathayat, G., Wang, X., Li, X., Wang, X., Wang, Y., Ning, Y., and Zhang, H.: The Asian monsoon over the past 640,000 years and ice age terminations, Nature, 534, 640-646, https://doi.org/10.1038/nature18591, 2016.

Counts, R. C., Murari, M. K., Owen, L. A., Mahan, S. A., and Greenan, M.: Late Quaternary chronostratigraphic framework of terraces and alluvium along the lower Ohio River, southwestern Indiana and western Kentucky, USA, Quaternary Science Reviews, 110, 72-91, https://doi.org/10.1016/j.quascirev.2014.11.011, 2015.

Dai, L., Fan, X., Jansen, J. D., and Xu, Q.: Landslides and fluvial response to landsliding induced by the 1933 Diexi earthquake, Minjiang River, eastern Tibetan Plateau, Landslides, 18, 3011-3025, https://doi.org/10.1007/s10346-021-01717-2, 2021.

Dai, L., Fan, X., Wang, D., Zhang, F., Yunus, A. P., Subramanian, S. S., Rogers, J. D., and Havenith, H.-B.: Electrical resistivity tomography revealing possible breaching mechanism of a Late Pleistocene long-lasted gigantic rockslide dam in Diexi, China, Landslides, 20, 1449-1463, https://10.1007/s10346-023-02048-0, 2023.

Deevey, E. S., Gross, M. S., Hutchinson, G. E., and Kraybill, H. L.: The natural 14C contents of materials from hard-water lakes, Proceedings of the National Academy of Sciences, 40, 285-288, https://doi.org/10.2307/88928, 1954.

Deng, B., Liu, S., Liu, S., Jansa, L., Li, Z., and Zhong, Y.: Progressive Indosinian N-S deformation of the Jiaochang structure in the Songpan-Ganzi fold-belt, Western China, PLoS One, 8, e76732, https://doi.org/10.1371/journal.pone.0076732, 2013.

do Prado, A. H., de Almeida, R. P., Galeazzi, C. P., Sacek, V., and Schlunegger, F.: Climate changes and the formation of fluvial terraces in central Amazonia inferred from landscape evolution modeling, Earth Surf Dynam, 10, 457-471, https://doi.org/10.5194/esurf-10-457-2022, 2022.

Duan, L.: The ancient barrier lake and geoenvironment, Diexi, Minjiang River, Chengdu University of Technology, Chengdu, 65 pp., 2002.

Duan, L., Wang, L., Yang, L., and Dong, X.: The ancient climatic evolution characteristic reflected by carbon and oxygen isotopes of carbonate in the ancient barrier lacustrine deposits, Diexi, Minjiang River, The Chinese Journal of Geological Hazard and Control, 13, 91-96, https://doi.org/10.3969/j.issn.1003-8035.2002.02.019, 2002.

Duller, G. A. T.: Distinguishing quartz and feldspar in single grain luminescence measurements, Radiation Measurements, 37, 161-165, https://10.1016/s1350-4487(02)00170-1, 2003.

Durcan, J. A., King, G. E., and Duller, G. A. T.: DRAC: Dose Rate and Age Calculator for trapped charge dating, Quaternary Geochronology, 28, 54-61, https://10.1016/j.quageo.2015.03.012, 2015.

Fan, X., Dai, L., Zhong, Y., Li, J., and Wang, L.: Recent research on the Diexi paleo-landslide: dam and lacustrine deposits upstream of the Minjiang River, Sichuan, China, Earth Science Frontiers, 28, 71-84, https://doi.org/10.13745/j.esf.sf.2020.9.2, 2021.

Fan, X., Xu, Q., van Westen, C. J., Huang, R., and Tang, R.: Characteristics and classification of landslide dams associated with the 2008 Wenchuan earthquake, Geoenvironmental Disasters, 4, 1-15, https://doi.org/10.1186/s40677-017-0079-8, 2017.

Fan, X., Yunus, A. P., Jansen, J. D., Dai, L., Strom, A., and Xu, Q.: Comment on 'Gigantic rockslides induced by fluvial incision in the Diexi area along the eastern margin of the Tibetan Plateau' by Zhao et al. (2019) Geomorphology 338, 27–42, Geomorphology, 402, https://doi.org/10.1016/j.geomorph.2019.106963, 2019.

Fan, X., Scaringi, G., Xu, Q., Zhan, W., Dai, L., Li, Y., Pei, X., Yang, Q., and Huang, R.: Coseismic landslides triggered by the 8th August 2017 Ms 7.0 Jiuzhaigou earthquake (Sichuan, China): factors controlling their spatial distribution and implications for the seismogenic blind fault identification, Landslides, 15, 967-983, https://doi.org/10.1007/s10346-018-0960-x, 2018.

Gao, H. S., Li, Z. M., Liu, F. L., Wu, Y. J., Li, P., Zhao, X., Li, F. Q., Guo, J., Liu, C. R., Pan, B. T., and Jia, H. T.: Terrace formation and river valley development along the lower Taohe River in central China, Geomorphology, 348, https://doi.org/10.1016/j.geomorph.2019.106885, 2020.

Gao, X. and Li, Y.: Comparison on the incision rate in the upper and middle reaches of Minjiang River, Resources and environment in the Yangtze Basin, 15, 517-521, https://doi.org/10.3969/j.issn.1004-8227.2006.04.020, 2006.

Giano, S. I. and Giannandrea, P.: Late Pleistocene differential uplift inferred from the analysis of fluvial terraces (southern Apennines, Italy), Geomorphology, 217, 89-105, https://doi.org/10.1016/j.geomorph.2014.04.016, 2014.

Gorum, T., Fan, X., van Westen, C. J., Huang, R. Q., Xu, Q., Tang, C., and Wang, G.: Distribution pattern of earthquake-induced landslides triggered by the 12 May 2008 Wenchuan earthquake, Geomorphology, 133, 152-167, https://doi.org/10.1016/j.geomorph.2010.12.030, 2011.

Grootes, P. M., Stulver, M., White, J. W. C., Johnsen, S. J., and Jouzel, J.: Comparison of oxygen records from the GISP2 and GRIP Greenland ice cores, Nature, 366, 6455, https://doi.org/10.1038/366552a0, 1993.

Guo, P.: Grain Size Characteristics and Optically stimulated luminescence Geochronology of Sediments in Diexi palaeo-dammed Lake, Upper Reaches of Minjiang River, China University of Geosciences, Beijing, 85 pp., 2018.

Guo, X., Sun, Z., Lai, Z., Lu, Y., and Li, X.: Optical dating of landslide-dammed lake deposits in the upper Yellow River, Qinghai-Tibetan Plateau, China, Quaternary

International, 392, 233-238, https://doi.org/10.1016/j.quaint.2015.06.021, 2016.
Gutiérrez, F. and Gutiérrez, M.: Landforms of the Earth, Springer International Publishing, Switzerland, 277 pp.2016.
Hewitt, K.: Disturbance regime landscapes: mountain drainage systems interrupted by large rockslides, Progress in Physical Geography: Earth and Environment, 30, 365-393, https://doi.org/10.1191/0309133306pp486ra, 2016.
Hewitt, K., Clague, J. J., and Orwin, J. F.: Legacies of catastrophic rock slope failures in mountain landscapes, Earth-Science Reviews, 87, 1-38, https://doi.org/10.1016/j.earscirev.2007.10.002, 2008.
Hewitt, K., Gosse, J., and Clague, J. J.: Rock avalanches and the pace of late Quaternary development of river valleys in the Karakoram Himalaya, Geological Society of America Bulletin, 123, 1836-1850, https://doi.org/10.1130/b30341.1, 2011.
Hou, Z., Li, Z., Qu, X., Gao, Y., Hua, L., Zheng, M., Li, S., and Yuan, W.: The uplift process of the Qinghai-Tibet Plateau since 0.5Ma - Evidence from hot water activity in the Gangdese belt, Science in China, 31, 27-33, 2001.
Hu, H.-P., Feng, J.-L., and Chen, F.: Sedimentary records of a palaeo-lake in the middle Yarlung Tsangpo: Implications for terrace genesis and outburst flooding, Quaternary Science Reviews, 192, 135-148, https://10.1016/j.quascirev.2018.05.037, 2018.
Huang, Z., Tang, R., and Liu, S.: Re-discussion on the Jiaochang Arcuate Structure, Sichuan Province, and the Seismogenic Structure for Diexi Earthquake in 1933, Earthquake Research in China, 17, 51-62, https://doi.org/CNKI:SUN:ZDZW.0.2003-01-005, 2003.
Jansen, J. D., Fabel, D., Bishop, P., Xu, S., Schnabel, C., and Codilean, A. T.: Does decreasing paraglacial sediment supply slow knickpoint retreat?, Geology, 39, 543-546, https://doi.org/10.1130/g32018.1, 2011.
Jansen, J. D., Nanson, G. C., Cohen, T. J., Fujioka, T., Fabel, D., Larsen, J. R., Codilean, A. T., Price, D. M., Bowman, H. H., May, J. H., and Gliganic, L. A.: Lowland river responses to intraplate tectonism and climate forcing quantified with luminescence and cosmogenic 10Be, Earth and Planetary Science Letters, 366, 49-58, https://doi.org/10.1016/j.epsl.2013.02.007, 2013.
Jiang, H., Zhong, N., Li, Y., Xu, H., Yang, H., and Peng, X.: Soft sediment deformation structures in the Lixian lacustrine sediments, eastern Tibetan Plateau and implications for postglacial seismic activity, Sedimentary Geology, 344, 123-134, https://doi.org/10.1016/j.sedgeo.2016.06.011, 2016.
Jiang, H., Mao, X., Xu, H., Yang, H., Ma, X., Zhong, N., and Li, Y.: Provenance and earthquake signature of the last deglacial Xinmocun lacustrine sediments at Diexi, East Tibet, Geomorphology, 204, 518-531, https://doi.org/10.1016/j.geomorph.2013.08.032, 2014.
Kang, S., Wang, X., and Lu, Y.: Quartz OSL chronology and dust accumulation rate changes since the Last Glacial at Weinan on the southeastern Chinese Loess Plateau, Boreas, 42, 815-829, https://10.1111/bor.12005, 2013.
Kang, S., Du, J., Wang, N., Dong, J., Wang, D., Wang, X., Qiang, X., and Song, Y.: Early Holocene weakening and mid- to late Holocene strengthening of the East

Asian winter monsoon, Geology, 48, 1043-1047, https://10.1130/g47621.1, 2020.
Kaplan, M. R., Wolfe, A. P., and Miller, G. H.: Holocene Environmental Variability in Southern Greenland Inferred from Lake Sediments, Quaternary Research, 58, 149-159, https://doi.org/10.1006/qres.2002.2352, 2002.
Keaveney, E. M. and Reimer, P. J.: Understanding the variability in freshwater radiocarbon reservoir offsets: a cautionary tale, Journal of Archaeological Science, 39, 1306-1316, https://doi.org/10.1016/j.jas.2011.12.025, 2012.
Kirby, E., Whipple, K. X., Burchfiel, B. C., Tang, W., Berger, G., Sun, Z., and Chen, Z.: Neotectonics of the Min Shan, China: Implications for mechanisms driving Quaternary deformation along the eastern margin of the Tibetan Plateau, Geological Society of America Bulletin, 112, 375-393, https://doi.org/10.1130/0016-7606(2000)112<375:NOTMSC>2.0.CO;2, 2000.
Korup, O. and Montgomery, D. R.: Tibetan plateau river incision inhibited by glacial stabilization of the Tsangpo gorge, Nature, 455, 786-789, https://doi.org/10.1038/nature07322, 2008.
Korup, O., Densmore, A. L., and Schlunegger, F.: The role of landslides in mountain range evolution, Geomorphology, 120, 77-90, https://doi.org/10.1016/j.geomorph.2009.09.017, 2010.
Korup, O., Clague, J. J., Hermanns, R. L., Hewitt, K., Strom, A. L., and Weidinger, J. T.: Giant landslides, topography, and erosion, Earth and Planetary Science Letters, 261, 578-589, https://doi.org/10.1016/j.epsl.2007.07.025, 2007.
Krivonogov, S. K., Takahara, H., Kuzmin, Y. V., Orlova, L. A., Timothy Jull, A. J., Nakamura, T., Miyoshi, N., Kawamuro, K., and Bezrukova, E. V.: Radiocarbon Chronology of the Late Pleistocene–Holocene Paleogeographic Events in Lake Baikal Region (Siberia), Radiocarbon, 46, 745-754, https://doi.org/10.1017/s0033822200035785, 2016.
Li, J. and Fang, X.: Study on the uplift and environmental change of the Qinghai-Tibet Plateau, Chinese Science Bulletin, 43, 1563-1574, https://doi.org/CNKI:SUN:KXTB.0.1998-15-000, 1998.
Liu, Y., Wang, X., Su, Q., Yi, S., Miao, X., Li, Y., and Lu, H.: Late Quaternary terrace formation from knickpoint propagation in the headwaters of the Yellow River, NE Tibetan Plateau, Earth Surface Processes and Landforms, 46, 2788-2806, https://doi.org/10.1002/esp.5208, 2021.
Lu, H., An, Z., Wang, X., Tan, H., Zhu, R., Ma, H., Li, Zhen, Miao, X., and Wang, X.: The staged uplift of the northeastern margin of the Qinghai-Tibet Plateau in the recent 14 Ma Geomorphic evidence, Science in China Series D Earth Sciences, 34, 855-864, https://doi.org/10.3321/j.issn:1006-9267.2004.09.008, 2004.
Luo, X., Yin, Z., and Yang, L.: Preliminary analysis on the development characteristics of river terraces and their relationship with ancient landslides in the upper reaches of Minjiang River, Quaternary Sciences, 39, 391-398, https://doi.org/10.11928/j.issn.1001-7410.2019.02.11, 2019.
Ma, J.: Sedimentary Characteristics of Outburst Deposits and Inversion of Outburst Flood Induced by the Diexi Paleo Dammed Lake of the Upper Minjiang River in China, China University of Geosciences, Beijing, 97 pp., 2017.

Ma, J., Chen, J., Cui, Z., Zhou, W., Liu, C., Guo, P., and Shi, Q.: Sedimentary evidence of outburst deposits induced by the Diexi paleolandslide-dammed lake of the upper Minjiang River in China, Quaternary International, 464, 460-481, https://doi.org/10.1016/j.quaint.2017.09.022, 2018.

Ma, Z., Peng, T., Feng, Z., Li, X., Song, C., Wang, Q., Tian, W., and Zhao, X.: Tectonic and climate controls on river terrace formation on the northeastern Tibetan Plateau: Evidence from a terrace record of the Huangshui River, Quaternary International, 656, 16-25, https://10.1016/j.quaint.2022.11.004, 2023.

Maddy, D., Demir, T., Bridgland, D. R., Veldkamp, A., Stemerdink, C., van der Schriek, T., and Westaway, R.: An obliquity-controlled Early Pleistocene river terrace record from Western Turkey?, Quaternary Research, 63, 339-346, https://10.1016/j.yqres.2005.01.004, 2005.

Malatesta, L. C., Finnegan, N. J., Huppert, K. L., and Carreño, E. I.: The influence of rock uplift rate on the formation and preservation of individual marine terraces during multiple sea-level stands, Geology, 50, 101-105, https://doi.org/10.1130/g49245.1, 2021.

Mao, X.: Preliminary study on lacustrine sediments at Diexi in the upper reach of the Minjiang River during the last deglaciation, China university of Geosciences, Beijing, 71 pp., 2011.

Miall, A. D.: Principles Of Sedimentary Basin, Springer, 616 pp.2000.

Molnar, P. and Houseman, G. A.: Rayleigh-Taylor instability, lithospheric dynamics, surface topography at convergent mountain belts, and gravity anomalies, Journal of Geophysical Research: Solid Earth, 118, 2544-2557, https://doi.org/10.1002/jgrb.50203, 2013.

Molnar, P., England, P., and Martinod, J.: Mantle dynamics, uplift of the Tibetan Plateau, and the Indian monsoon, Journal of Geophysical Research: Solid Earth, 118, 2544-2557, https://doi.org/10.1029/93RG02030, 1993.

Montgomery, D. R., Hallet, B., Yuping, L., Finnegan, N., Anders, A., Gillespie, A., and Greenberg, H. M.: Evidence for Holocene megafloods down the tsangpo River gorge, Southeastern Tibet, Quaternary Research, 62, 201-207, https://10.1016/j.yqres.2004.06.008, 2004.

Murray, A. S. and Wintle, A. G.: Luminescence dating of quartz using an improved single-aliquot regenerative-dose protocol, Radiation Measurements, 32, 57-73, https://doi.org/10.1016/S1350-4487(99)00253-X, 2000.

Narzary, B., Singh, A. K., Malik, S., Mahadev, and Jaiswal, M. K.: Luminescence chronology of the Sankosh river terraces in the Assam-Bhutan foothills of the Himalayas: Implications to climate and tectonics, Quaternary Geochronology, 72, https://10.1016/j.quageo.2022.101364, 2022.

Oh, J. S., Seong, Y. B., Hong, S., and Yu, B. Y.: Paleo-shoreline changes in moraine dammed lake Khagiin Khar, Khentey Mountains, Central Mongolia, Journal of Mountain Science, 16, 1215-1230, https://doi.org/10.1007/s11629-019-5445-4, 2019.

Okuno, J., Nakada, M., Ishii, M., and Miura, H.: Vertical tectonic crustal movements along the Japanese coastlines inferred from late Quaternary and recent relative sea-level changes, Quaternary Science Reviews, 91, 42-61, https://doi.org/10.1016/j.quascirev.2014.03.010, 2014.

Pan, B., Burbank, D., Wang, Y., Wu, G., Li, J., and Guan, Q.: A 900 k.y. record of strath terrace formation during glacial-interglacial transitions in northwest China, Geology, 31, https://doi.org/10.1130/g19685.1, 2003.

Pan, B., Hu, X., Gao, H., Hu, Z., Cao, B., Geng, H., and Li, Q.: Late Quaternary river incision rates and rock uplift pattern of the eastern Qilian Shan Mountain, China, Geomorphology, 184, 84-97, https://doi.org/10.1016/j.geomorph.2012.11.020, 2013.

Prescott, J. R. and Hutton, J. T.: Cosmic ray contributions to dose rates for luminescence and ESR dating: large depths and long-term time variations, Radiation Measurements, 23, 497-500, https://10.1016/1350-4487(94)90086-8, 1994.

Rees-Jones, J.: Optical dating of young sediments using fine-grain quartz, Ancient TL, 13, 9-14, 1995.

Reimer, P. J., Austin, W. E. N., Bard, E., Bayliss, A., Blackwell, P. G., Bronk Ramsey, C., Butzin, M., Cheng, H., Edwards, R. L., Friedrich, M., Grootes, P. M., Guilderson, T. P., Hajdas, I., Heaton, T. J., Hogg, A. G., Hughen, K. A., Kromer, B., Manning, S. W., Muscheler, R., Palmer, J. G., Pearson, C., van der Plicht, J., Reimer, R. W., Richards, D. A., Scott, E. M., Southon, J. R., Turney, C. S. M., Wacker, L., Adolphi, F., Büntgen, U., Capano, M., Fahrni, S. M., Fogtmann-Schulz, A., Friedrich, R., Köhler, P., Kudsk, S., Miyake, F., Olsen, J., Reinig, F., Sakamoto, M., Sookdeo, A., and Talamo, S.: The IntCal20 Northern Hemisphere Radiocarbon Age Calibration Curve (0–55 cal kBP), Radiocarbon, 62, 725-757, https://doi.org/10.1017/rdc.2020.41, 2020.

Schumm, S. A. and Parker, R. S.: Implications of Complex Response of Drainage Systems for Quaternary Alluvial Stratigraphy, Nature, 243, 99-100, https://doi.org/10.1038/physci243099a0, 1973.

Shen, M.: Earthquake Information Study For Paleo-dammed Lake At Minjiang River Upstream, Chengdu University of Technology, Chengdu, 1-129 pp., 2014.

Shi, W.: Impact of tectonic activities and climate change on the lacustrine sediments in the eastern Tibet during the last deglaciation, Institute of Geology, China Earthquake Administrator, Beijing, 135 pp., 2020.

Shi, Y., Li, J., Li, B., Yao, T., Wang, S., Li, S., Cui, Z., Wang, F., Pan, B., Fang, X., and Zhang, Q.: Uplift of the Qinghai—Xizang (Tibetan) Plateau and east Asia environmental change during late cenozoic, ACTA GEOGRAPHICA SINICA, 12-22, https://doi.org/10.3321/j.issn:0375-5444.1999.01.002, 1999.

Singh, A. K., Pattanaik, J. K., Gagan, and Jaiswal, M. K.: Late Quaternary evolution of Tista River terraces in Darjeeling-Sikkim-Tibet wedge: Implications to climate and tectonics, Quaternary International, 443, 132-142, https://doi.org/10.1016/j.quaint.2016.10.004, 2017.

Srivastava, P., Tripathi, J. K., Islam, R., and Jaiswal, M. K.: Fashion and phases of late Pleistocene aggradation and incision in the Alaknanda River Valley, western Himalaya, India, Quaternary Research, 70, 68-80, https://doi.org/10.1016/j.yqres.2008.03.009, 2017.

Tang, R., Jiang, N., and Liu, S.: Recognition of the Geological Setting and the Seismogenic Condition for the Diexi Magnitude 7.5 Earthquake, Journal of seisnological research, 6, 327-338, https://doi.org/CNKI:SUN:DZYJ.0.1983-03-011, 1983.

Vásquez, A., Flores-Aqueveque, V., Sagredo, E., Hevia, R., Villa-Martínez, R., Moreno, P. I., and Antinao, J. L.: Evolution of Glacial Lake Cochrane During the Last Glacial Termination, Central Chilean Patagonia (~47°S), Frontiers in Earth Science, 10, 1-19, https://doi.org/10.3389/feart.2022.817775, 2022.

Wang, H., Wang, P., Hu, G., Ge, Y., and Yuan, R.: An Early Holocene river blockage event on the western boundary of the Namche Barwa Syntaxis, southeastern Tibetan Plateau, Geomorphology, 395, 1-20, https://doi.org/10.1016/j.geomorph.2021.107990, 2021a.

Wang, J., Yang, S. T., Lou, H. Z., Liu, H. P., Wang, P. F., Li, C. J., and Zhang, F.: Impact of lake water level decline on river evolution in Ebinur Lake Basin (an ungauged terminal lake basin), Int J Appl Earth Obs, 104, 1-14, https://doi.org/10.1016/j.jag.2021.102546, 2021b.

Wang, L., Wang, X., Xu, X., and Cui, J.: What happened on the upstream of Minjiang River in Sichuan Province 20,000 years ago, Earth Science Frontiers, 14, 189-196, https://www.earthsciencefrontiers.net.cn/CN/Y2007/V14/I6/189, 2007.

Wang, L., Yang, L., Wang, X., and Duan, L.: Discovery of huge ancient dammed lake on upstream of Minjiang River in Sichuan , China, Journal of Chengdu University of Technology, 32, 1-11, 2005a.

Wang, L., Yang, L., Wang, X., and Duan, L.: Discovery of huge ancient dammed lake on upstream of Minjiang River in Sichuan , China, Journal of Chengdu University of Technology (Science & Technology Edition), 32, 1-11, https://doi.org/CNKI:SUN:CDLG.0.2005-01-001, 2005b.

Wang, L., Wang, X., Xu, X., Cui, J., Shen, J., and Zhang, Z.: Significances of studying the diexi paleo dammed lake at the upstream of minjiang river, sichuan, China, Quaternary Sciences, 32, 998-1010, https://doi.org/10.3969/j.issn.1001-7410.2012.05.16, 2012.

Wang, L., Wang, X., Shen, J., Xu, X., Cui, J., Zhang, Z., and Zhou, Z.: The effect of evolution of Diexi ancient barrier lake in the upper Mingjiang River on the Chengdu Plain in Sichuan, China, Journal of Chengdu University of technology, 47, 1-15, https://doi.org/10.3969/j.issn.1671-9727.2020.01.01, 2020a.

Wang, L., Wang, X., Shen, J., Yin, G., Cui, J., Xu, X., Zhang, Z., Wan, T., and Wen, L.: Late Pleistocene environmental information on the Diexi paleo-dammed lake of the upper Minjiang River in the eastern margin of the Tibetan Plateau, China, Journal of Mountain Science, 17, 1172-1187, https://10.1007/s11629-019-5573-x, 2020b.

Wang, P., Zhang, B., Qiu, W., and Wang, J.: Soft-sediment deformation structures from the Diexi paleo-dammed lakes in the upper reaches of the Minjiang River, east Tibet, Journal of Asian Earth Sciences, 40, 865-872, https://doi.org/10.1016/j.jseaes.2010.04.006, 2011.

Wang, X.: The Environment Geological Information in the Sediments of Diexi Ancient

Dammed Lake on the upstream of Mingjiang River in Sichuan Province, China, Chengdu University of Technology, Chengdu, 116 pp., 2009.

Wang, X., Li, C., Lv, L., and Dong, J.: Analysis of the late Quaternary activity along the Wenchuan-Maoxian fault-middle of the back-range fault at the Longmenshan fault zone, Seismology and Geology, 39, 572-586, https://doi.org/10.3969/j.issn.0253-4967.2017.03.010, 2017.

Wang, X., Li, Y., Yuan, Y., Zhou, Z., and Wang, L.: Palaeoclimate and palaeoseismic events discovered in Diexi barrier lake on the Minjiang River, China, Natural Hazards and Earth System Sciences, 14, 2069-2078, https://doi.org/10.5194/nhess-14-2069-2014, 2014.

Wang, Y., Cheng, H., Edwards, R. L., An, Z., Wu, J., Shen, C.-C., and Dorale, J. A.: A high-resolution absolute-dated late Pleistocene monsoon record from Hulu cave, China, Science, 294, 2345-2348, https://doi.org/10.1126/science.1064618, 2001.

Wang, Y., Cheng, H., Edwards, R. L., Kong, X., Shao, X., Chen, S., Wu, J., Jiang, X., Wang, X., and Wang, Z.: Millennial- and orbital-scale changes in the East Asian monsoon over the past 224,000 years, Nature, 451, 1090-1093, https://doi.org/10.1038/nature06692, 2008.

Westaway, R. and Bridgland, D.: Late Cenozoic uplift of southern Italy deduced from fluvial and marine sediments: Coupling between surface processes and lower-crustal flow, Quaternary International, 175, 86-124, https://doi.org/10.1016/j.quaint.2006.11.015, 2007.

Wintle, A. G. and Murray, A. S.: A review of quartz optically stimulated luminescence characteristics and their relevance in single-aliquot regeneration dating protocols, Radiation Measurements, 41, 369-391, https://10.1016/j.radmeas.2005.11.001, 2006.

Wu, L., Zhao, D. J., Zhu, J., Peng, J., and Zhou, Y.: A Late Pleistocene river-damming landslide, Minjiang River, China, Landslides, 17, 433-444, https://doi.org/10.1007/s10346-019-01305-5, 2019.

Xu, H., Chen, J., Cui, Z., and Chen, R.: Sedimentary facies and depositional processes of the Diexi Ancient Dammed Lake, Upper Minjiang River, China, Sedimentary Geology, 398, https://10.1016/j.sedgeo.2019.105583, 2020.

Yang, F., Fan, X., Siva Subramanian, S., Dou, X., Xiong, J., Xia, B., Yu, Z., and Xu, Q.: Catastrophic debris flows triggered by the 20 August 2019 rainfall, a decade since the Wenchuan earthquake, China, Landslides, 18, 3197-3212, https://doi.org/10.1007/s10346-021-01713-6, 2021.

Yang, N., Zhang, Y., Meng, H., and Zhang, H.: Study of the Minjiang River terraces in the western Sichuan Plateau, Journal of Geomechanics, 9, 363-370, https://doi.org/10.3969/j.issn.1006-6616.2003.04.008, 2003.

Yang, W.: Research of Sedimentary Record in Terraces and Climate Vary in the Upper Reaches of Minjiang River, China, Chengdu University of Technology, Chengdu, 2005.

Yang, W., Zhu, L., Zhang, Y., and Kan, A.: Sedimentary evolution of a dammed paleolake in the Maoxian basin on the upper reach of Minjiang River, Sichuan, China, Marine Geology Frontiers, 27, 35-40, https://doi.org/CNKI:SUN:HYDT.0.2011-05-007, 2011.

Yang, W., Zhu, L., Zheng, H., Xiang, F., Kan, A., and Luo, L.: Evoluton of a dammed palaeolake in the Quaternary Diexi basin on the upper Minjiang River, Sichuan, China, Geological Bulletion of China, 27, 605-610, https://doi.org/10.3969/j.issn.1671-2552.2008.05.003, 2008.

Yang, Y., Li, B., Yin, Z., and Zhang, Q.: The Formation and Evolution of Landforms in the Xizang Plateau, ACTA GEORAPHICA SINICA, 76-87, https://doi.org/10.11821/xb198201009, 1982.

Yoshikawa, T., KaizukaYoko, S., and Ota, O.: Mode of crustal movement in the late Quaternary on the southeast coast of Shikoku, southwestern Japan, Geographical Review of Japan, 37, 627-648, https://doi.org/10.4157/grj.37.627, 1964.

Yu, Y., Wang, X., Yi, S., Miao, X., Vandenberghe, J., Li, Y., and Lu, H.: Late Quaternary aggradation and incision in the headwaters of the Yangtze River, eastern Tibetan Plateau, China, GSA Bulletin, 134, 371-388, https://doi.org/10.1130/b35983.1, 2021.

Yuan, G. and Zeng, Q.: Glacier-dammed lake in Southeastern Tibetan Plateau during the Last Glacial Maximum, Journal Geological Society of India, 79, 295-301, https://10.1007/s12594-012-0041-z, 2012.

Zhang, B., Wang, P., and Wang, J.: Discussion of the Origin of the Soft-Sediment Deformation Structures in Paleo-dammed Lake Sediments in the Upper Reaches of the Minjiang River, Journal of Seismological Research, 34, 67-74, https://doi.org/10.3969/j.issn.1000-0666.2011.01.011, 2011.

Zhang, S.: Characteristics and Geological Significance of the Late Pleistocene Lacustrine Sediments in Diexi, Sichuan, China University of Geosciences, Beijing, 76 pp., 2019.

Zhang, Y., Zhu, L., Yang, W., Luo, H., Jiang, L., He, D., and Liu, J.: High Resolution Rapid Climate Change Records of Lacustrine Deposits of Diexi Basin in the Eastern Margin of Qinghai-Tibet Plateau, 40–30 ka BP, Earth Science Frontiers, 16, 91-98, https://doi.org/10.1016/s1872-5791(08)60106-2, 2009.

Zhao, X., Deng, Q., and Chen, S.: Tectonic geomorphology of the Minshan uplift in western Sichuan, southwestern China, Seismology and Geology, 16, 429-439, https://doi.org/CNKI:SUN:DZDZ.0.1994-04-017, 1994.

Zhong, N.: Earthquake and Provenance Analysis of the Lacustrine Sediments in the Upper Reaches of the Min River during the Late Pleistocene, Institute of Geology, China Earthquake Administration, Beijing, 193 pp., 2017.

Zhong, Y., Fan, X., Dai, L., Zou, C., Zhang, F., and Xu, Q.: Research on the Diexi Giant Paleo-Landslide along Minjiang River in Sichuan, China, Progress in Geophysics, 36, 1784-1796, https://doi.org/10.6038/pg2021EE0367, 2021.

Zhou, R., Pu, X., He, Y., Li, X., and Ge, T.: Recent activity of Minjiang fault zone, uplift of Minshan block and their relationship with seismicity of Sichuan, Seismology and Geology, 22, 285-294, https://doi.org/CNKI:SUN:DZDZ.0.2000-03-009, 2000.

Zhu, J.: A preliminary study on the upper reaches of Minjiang River Terrace, Chengdu University of Technology, Chengdu, 73 pp., 2014.

Zhu, S., Wu, Z., Zhao, X., and Keyan, X.: Glacial dammed lakes in the Tsangpo River during late Pleistocene, southeastern Tibet, Quaternary International, 298, 114-122, https://10.1016/j.quaint.2012.11.004, 2013.